



Project funded by the European Commission under the 6th (EC) RTD Framework Programme (2002- 2006) within the framework of the specific research and technological development programme "Integrating and strengthening the European Research Area"



Project UpWind

Contract No.:
019945 (SES6)

"Integrated Wind Turbine Design"



Impact of Drivetrain on Wind Farm VAR Control

AUTHOR:	Parag Vyas, Emad Ahmed
AFFILIATION:	GE Global Research
ADDRESS:	Freisinger Landstr 50, Munich, Germany
TEL.:	+49 89 5528 3414
EMAIL:	parag.vyas@ge.com , emad.ahmed@ge.com
FURTHER AUTHORS:	
REVIEWER:	Project members
APPROVER:	

Document Information

DOCUMENT TYPE	Deliverable D5.9.1
DOCUMENT NAME:	Impact of Drivetrain on Wind Farm VAR Control
REVISION:	1.0
REV.DATE:	26 October 2010
CLASSIFICATION:	R0: General Public
STATUS:	S0: Approved/Released

STATUS, CONFIDENTIALITY AND ACCESSIBILITY							
Status			Confidentiality			Accessibility	
S0	Approved/Released	X	R0	General public	X	Private web site	
S1	Reviewed		R1	Restricted to project members		Public web site	X
S2	Pending for review		R2	Restricted to European. Commission		Paper copy	
S3	Draft for comments		R3	Restricted to WP members + PL			
S4	Under preparation		R4	Restricted to Task members +WPL+PL			

PL: Project leader **WPL:** Work package leader **TL:** Task leader

Contents

Executive Summary	8
1. GE Wind Turbine/Generator Modelling	10
1.1 Modelling Overview.....	10
1.2 Full Converter WTGs	10
1.3 WTG Model Structure	11
1.4 WTG Dynamic Model.....	12
1.4.1 Generator/Converter Model	12
1.4.2 Electrical (Converter) Control Model	12
1.4.3 Wind Turbine and Turbine Control Model	12
2. Test System Description	13
2.1 Wind Turbine Generator Modelling for Load Flow	13
2.2 Test System Parameters	14
2.3 Impedance Allocation of Test System Components	15
3. Wind Farm VAR Control for WTGs with Power Electronics for Grid Interface	17
3.1 Wind Farm VAR Design Guidelines.....	17
3.1.1 WTG Voltage Control Loop	18
3.1.2 Reactive Power Control Loop	18
3.1.3 Wind Farm VAR Control Loop.....	19
3.2 Wind VAR Control Parameters Determination.....	19
3.2.1 Response to a WTG Step Reactive Power Command	19
3.2.2 Response to a Step Change of Regulated Voltage	21
3.3 Simulation Results with One and Two Aggregate WTGs Model with DFIG.....	25
3.3.1 Test Cases	26
3.3.2 Results Summary and Conclusions	26
4. WTG Synchronous Machine	30
4.1 Static-Type Excitation System	30
4.1.1 Performance of Static-Type Excitation System.....	30
4.1.2 Wind Farm VAR Control using WTG Voltage Control.....	36
4.1.3 Tuning the PI Controller	36
4.1.4 Test Cases	38
4.1.5 Results Summary and Conclusions	39
4.1.6 Wind Farm VAR Control with WTG Reactive Power Control Implementation.....	42
4.1.7 Reactive Power Control Loop	42
4.1.8 Wind Farm VAR Control Loop.....	44
4.1.9 Test Cases and Results	48
4.2 Brushless-Type Excitation System	50
4.2.1 Performance of Brushless-Type Excitation System.....	50
4.2.2 Wind Farm VAR Control using WTG Voltage Control.....	54
4.2.3 Test Cases and Conclusions	56
4.2.4 Wind Farm VAR Control with WTG Reactive Power Control Implementation.....	59
4.2.5 Test Cases and Results	63
5. Summary	65
6. Acknowledgements	66
7. References.....	66

List of Figures

Figure 1-1. GE 1.5 and 3.6 WTG major components.....	10
Figure 1-2. Full converter WTG major components.	11
Figure 1-3. GE WTG dynamic model structure.....	12
Figure 2-1. Wind turbine load flow model.	13
Figure 2-2. Test System.....	14
Figure 2-3. Impedance allocation of system components with all WTGs online.	16
Figure 2-4. Impedance allocation of system components with half of WTGs online.....	16
Figure 3-1. Wind farm VAR control block diagram.	17
Figure 3-2. System response to a step reactive power command (Q_{cmd}) for different SCRs.....	21
Figure 3-3. System response to a step change of regulated voltage for different SCRs (324 MW, all WTGs are connected at full power).....	23
Figure 3-4. System response to a step change of regulated voltage for different SCRs with $F_n=1.0$ (162 MW, half of WTGs are connected at full power).	24
Figure 3-5. System response to a step change of regulated voltage for different SCRs with $F_n=0.5$ (162MW, half of WTGs are connected at full power).	25
Figure 3-6. Wind farm representation and the VAR control structure.	26
Figure 4-1. Static excitation control block diagram.....	30
Figure 4-2. Open loop Bode diagram of the static excitation system.....	32
Figure 4-3. Closed loop Bode diagram of the static excitation system.....	33
Figure 4-4. Static excitation system response with all WTGs in service (324 MW).	34
Figure 4-5. Static excitation system response with half of the WTGs in service (162 MW).	35
Figure 4-6. Wind farm VAR control block diagram with static excitation system.....	36
Figure 4-7. System response with VAR control for different PI controller settings with half of the WTGs in service (static excitation, SCR=5).	38
Figure 4-8. Wind farm VAR control block diagram for synchronous machine WTG.	42
Figure 4-9. System response with static excitation of synchronous WTG to a 0.3 pu step change of the reference WTG reactive power (324 MW, all WTGs in service).	44
Figure 4-10. System response with static excitation of synchronous WTG to a regulated voltage step change (v_{ref}) for different SCRs (all WTGs in service with $F_n=1$).	46
Figure 4-11. System response with static excitation of synchronous WTG to a regulated voltage step change (v_{ref}) for different SCRs (half of WTGs in service with $F_n=0.5$).	47
Figure 4-12. Brushless excitation control block diagram.....	50
Figure 4-13. Open loop Bode diagram of the brushless excitation system.....	51
Figure 4-14. Closed loop Bode diagram of the brushless excitation system.....	52
Figure 4-15. Brushless excitation system response with all WTGs in service (324 MW).	53
Figure 4-16. Brushless excitation system response with half of the WTGs in service (162 MW).	54
Figure 4-17. Wind farm VAR control block diagram with brushless excitation system.	55
Figure 4-18. System response with VAR control for different PI controller settings with half of the WTGs in service (brushless excitation, SCR=5).	56
Figure 4-19. A voltage collapse case with half of WTGs for system SCR 20.....	57
Figure 4-20. System response with brushless excitation of synchronous WTG to a 0.3 pu step change of the reference WTG reactive power (324 MW, all WTGs are in service).....	60

Figure 4-21. System response with brushless excitation of synchronous WTG to a regulated voltage step change (v_{rfg}) for different SCRs (all WTGs in service with $F_n=1$). 61

Figure 4-22. System response with brushless excitation of synchronous WTG to a regulated voltage step change (v_{rfg}) for different SCRs (half of WTGs in service with $F_n=0.5$). 62

List of Tables

Table 2-1. WTG load flow data	13
Table 2-2. Wind farm system data	15
Table 2-3. MV and HV system cable configurations.....	15
Table 2-4. Impedance contribution range of different components of the test system.....	16
Table 3-1 VAR Control Parameters with DFIG machine for Different SCRs.....	19
Table 3-2. Summary results of considered test cases for DFIG WTG	29
Table 4-1. Parameters of the control block diagram of the static excitation system	31
Table 4-2. Variation of F_{sc} value for different system SCRs with different number of WTGs.....	36
Table 4-3. VAR control parameters with static excitation system.....	36
Table 4-4. Summary results of test cases for VAR control with static excitation of synchronous WTG implementing only voltage control	41
Table 4-5 WTG reactive power control loop parameters with static excitation system	43
Table 4-6 Wind VAR control loop parameters with static excitation system	45
Table 4-7. Summary results of test cases for VAR control with static excitation of synchronous WTG implementing reactive power control.....	49
Table 4-8. Parameters of control block diagram of brushless excitation system.	50
Table 4-9. VAR control parameters with brushless excitation system	55
Table 4-10. Summary results of test cases for VAR control with brushless excitation of synchronous WTG implementing only voltage control	58
Table 4-11. Wind farm VAR control parameters with reactive power control implementation with brushless excitation system	59
Table 4-12. Summary results of test cases for VAR control with brushless excitation of synchronous WTG implementing reactive power control	64

Glossary

DFIG	Doubly Fed Induction Generator
HV	High Voltage
MV	Medium Voltage
POI	Point Of Interconnection
PSLF	Positive Sequence Load Flow
PV bus	Generator bus
SCR	Short Circuit Ratio
VAR	Volt ampere reactive
WTG	Wind Turbine Generator

Executive Summary

The Upwind project is concerned with all aspects of the next generation of wind turbines. As turbine power ratings increase into the multi-MW range, the design of drivetrains may feature technologies not common to today's wind turbines. Example concepts are hydrodynamic viscously coupled gearboxes and superconducting electrical machines.

To interconnect a wind farm to a grid, utilities will require the wind farm to maintain the voltage at the point of interconnection (POI). The voltage control can be performed by actively regulating the reactive power from the wind turbine generator. This is called wind farm VAR control.

Of increasing concern as wind penetration increases, is the performance of wind farms with respect to voltage control functions performed using reactive power modulation, and the performance to voltage dip events on the network. The ability of wind turbines to ride through voltages dips depends on wind turbine technology and the way in which the turbine control system reacts.

The Upwind task reported here is aimed at developing a case study for a future large-scale offshore wind farm and evaluating the impact of the choice of drivetrain on wind farm-grid performance in terms of voltage control. Fast control of wind farms is conducted through a supervisory VAR controller, which performs some voltage regulation by sending reference reactive power commands to the turbines. This study investigates:

- The interaction of voltage regulation with and without high bandwidth power electronics within the system. Accordingly, different associated wind turbine generator types are considered depending on the drivetrain choice.
- Extending the “reach”, i.e., the point on the system where the voltage can be controlled. For offshore wind farms, this determines the effect of long cables to and how well the voltage is controlled.
- Voltage compensation under system disturbances.
- The effect of grid strength level and the number of connected wind turbines on tuning the wind farm VAR control. The dominant factors that affect the control performance will be characterized.
- Setting up a criterion for evaluating the performance of the wind farm VAR control.

A large-scale offshore wind farm was the focus of this study where the turbine rating and size of the farm are in line with the future needs of the industry. The electrical design considered a 324 MW wind farm with individual 6 MW wind turbines. The medium voltage (MV) collector feeders and high voltage (HV) subsea transmission cables were designed based on the Upwind project work package WP9.4.2 [1].

Design guidelines of the VAR control are presented. A test system is considered and simulations for different scenarios are carried out using GE's PSLF load flow and dynamic simulation software to validate the design guidelines and characterize the control performance under different system and wind farm configurations.

The study considers the sensitivity of grid parameters to the system voltage response performance. The grid short circuit ratio (SCR) is found to have a significant impact on the response dynamics and any form of controller must be designed and tuned according to the prevailing SCR. In addition monitoring the number of connected Wind Turbine-Generators (WTGs) is found to be important for updating the control parameters to maintain the desired system voltage response.

The comparison between drivetrains with power converter interfaces, either in DFIG configuration (such as that found on GE 1.5 and GE 3.6 WTGs), or full power converters (as is the case with the GE 2.5), and with purely synchronous machines coupled directly to the grid, shows that with well-tuned control parameters, the VAR control performance with the

conventional synchronous machines could have similar time responses to that obtained with power electronic grid interfaces.

1. GE Wind Turbine/Generator Modelling

Existing and future turbine concepts are modelled in this report. The existing turbine concepts are based on existing GE products, which has two types of wind turbine generators. The first has a partially rated converter in doubly fed induction generator configuration (GE1.5 and GE3.6). The second type (GE2.5) has a rating of 2.5 MW and has a full converter for grid interface.

1.1 Modelling Overview

A simple schematic of an individual GE 1.5 or 3.6 MW Wind Turbine-Generator (WTG) is shown in Figure 1-1. Physically, the GE wind turbine generator 1.5 or 3.6 machines are a relatively conventional wound rotor induction (WRI) machine. However, the key distinction is that this machine is equipped with a solid-state voltage-source converter AC excitation system. The AC excitation is supplied through an AC-DC-AC converter. For the GE 3.6 machine, the converter is connected as shown via a transformer. For the GE 1.5 machine, it is connected directly at the stator winding. Machines of this structure are termed doubly fed induction generators (DFIG), and have significantly different dynamic behaviour than either conventional synchronous or induction machines [2].

The fundamental frequency electrical dynamic performance of this type of GE WTG is completely dominated by the converter. Conventional aspects of generator performance related to internal angle, excitation voltage, and synchronism are largely irrelevant. For all GE machines, the control of active and reactive power is handled by fast, high bandwidth regulators within the converter controls. The time responses of the converter regulators are sub-cycle, and as such can be greatly simplified for simulation of bulk power system dynamic performance. The AC system dynamic response of all these GE machines is similar, and for stability simulations, can be modelled with the same structure. Therefore, the proposed baseline 6 MW wind turbine in this study will have the same structure.

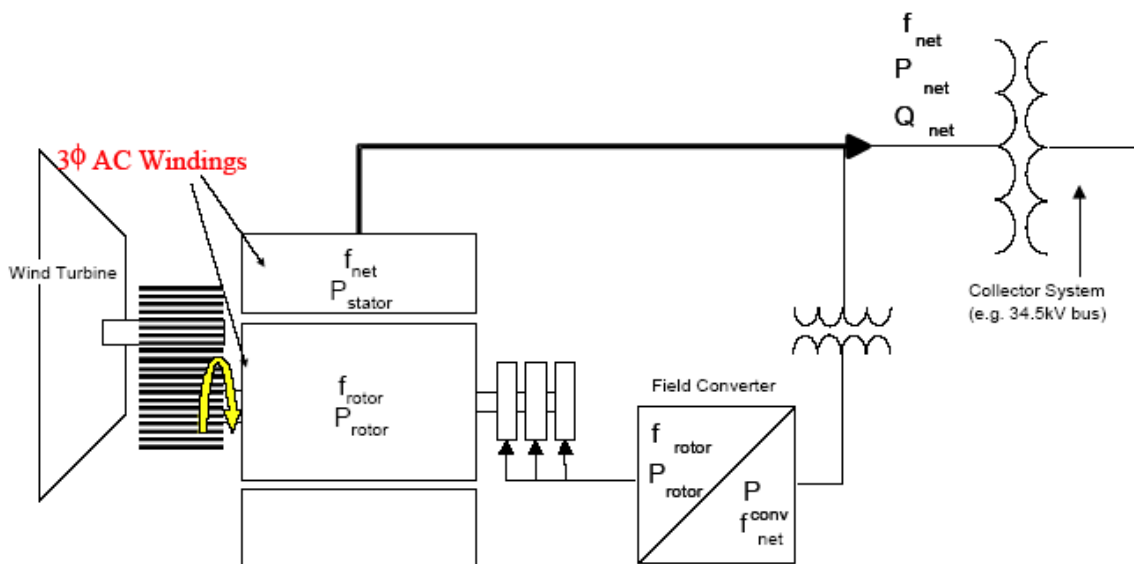


Figure 1-1. GE 1.5 and 3.6 WTG major components.

1.2 Full Converter WTGs

The GE 2.5 MW is another type of WTG that utilizes power electronic converters. It is a conventional synchronous generator connected to the power grid through a full converter as shown in Figure 1-2. The configuration decouples the generator speed from the power system frequency and allows for a wide range of variable speed operation. The converter grid side corresponds to the WTG terminals.

With the implementation of full converter WTG, the grid dynamic performance would be dominated by the converter controls for controlling the active and reactive power. This is handled by fast, high bandwidth regulators within the converter controls. The turbine control is also the same as that used for DFIG, therefore, the full converter WTG would have the same

dynamic model basis as in the DFIG. Accordingly, it can be claimed that the VAR control performance of the full converter WTG would be similar to that provided by the DFIG.

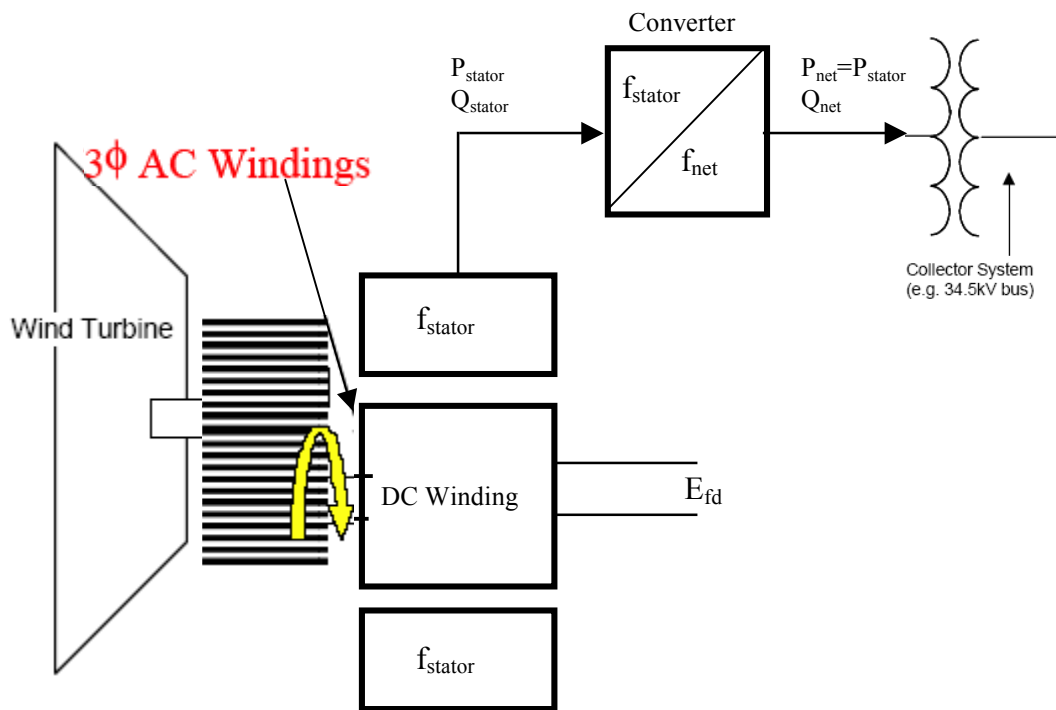


Figure 1-2. Full converter WTG major components.

1.3 WTG Model Structure

The primary control objective of the wind VAR is to maintain the voltage at the point of interconnection (POI) as steady as possible under different system disturbances such as grid transients outside the wind farm. The voltage variation at this point should be small at as wide a range of frequencies as possible. This can be achieved through the dynamic behaviour of the WTG equipment in a fashion that is similar to conventional generators. Figure 1-3 shows the structure of the GE WTG dynamic model. It has three main device models:

- 1) Generator/converter model (injects real and reactive current into network in response to control commands).
- 2) Electrical control model (includes closed loop reactive power controls including the Wind VAR system).
- 3) Turbine and turbine control model (mechanical controls, including blade pitch control and power command (torque command in the actual equipment) to converter; over/under speed trips; rotor inertia equation; wind power as a function of wind speed, blade pitch, and rotor speed).

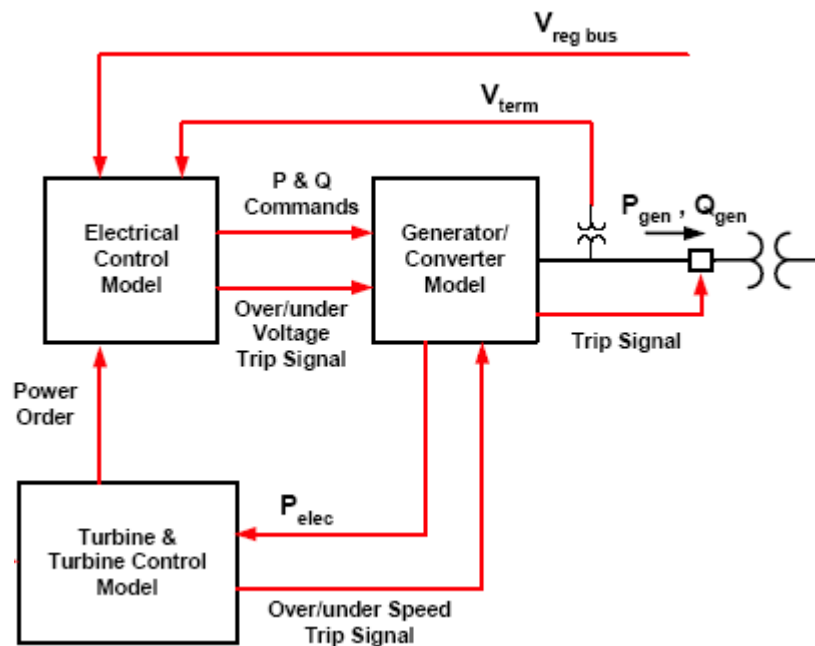


Figure 1-3. GE WTG dynamic model structure.

1.4 WTG Dynamic Model

1.4.1 Generator/Converter Model

This model is the equivalent of the generator and the field converter and provides the interface between the WTG and the network. Unlike a conventional generator model, it contains no mechanical state variables for the machine rotor, which are included in the turbine model.

Furthermore, unlike conventional generator models, all of the flux dynamics have been eliminated to reflect the rapid response to the higher level commands from the electrical controls through the converter. The net result is an algebraic, controlled-current source that computes the required injected current into the network in response to the flux and active current commands from the electrical control model.

1.4.2 Electrical (Converter) Control Model

This model dictates the active and reactive power to be delivered to the system based on inputs from the turbine model and from the supervisory VAR control. A wind turbine generator (WTG) usually has a voltage control loop that regulates the wind turbine generator terminal voltage. In addition, there is a reactive power control loop that regulates the reactive power output. The reactive power command can be a set point or can be supplied by system supervisory VAR control. It can also be determined by a power factor regulator.

The electrical controller model is a simplified representation of the converter control system. This model monitors the WTG reactive power and terminal voltage to compute the field command to the WTG model.

1.4.3 Wind Turbine and Turbine Control Model

The wind turbine model provides a simplified representation of a very complex electro-mechanical system. In simple terms, the function of the wind turbine is to extract as much power from the available wind as possible without exceeding the rating of the equipment. The wind turbine model represents the relevant controls and mechanical dynamics of the wind turbine. It implements a moderately complex algebraic relationship that governs the mechanical shaft power that is dependent on wind velocity, rotor speed and blade pitch angle.

The turbine control model sends a power command to the electrical control model, requesting that the converter deliver a specified power to the grid. The practical implication of the turbine control is that when the available wind power is above the equipment rating, the blades are pitched to limit the mechanical power delivered to the shaft to the equipment rating. When the

available wind power is less than rated, the blades are set at minimum pitch to maximize the mechanical power. The blade position actuators are rate limited and there is a time constant associated with the translation of blade angle to mechanical output. The dynamics of the pitch control are moderately fast, and can have significant impact on dynamic simulation results. The turbine control acts to smooth out electrical power fluctuations due to variations in shaft power. This is achieved by allowing the machine speed to vary around reference speed where the inertia of the machine functions as a buffer to mechanical power variations.

2. Test System Description

2.1 Wind Turbine Generator Modelling for Load Flow

Wind farms normally consist of a large number of individual wind turbine generators (WTGs). The wind farm model may consist of a detailed representation of each WTG and the collector system. Alternatively, the simpler model shown in Figure 2-1 is adequate for most bulk transmission system studies. This model consists of a single equivalent WTG and unit transformer with MVA ratings equal to N times the individual device ratings, where N is the number of WTGs in the wind farm (or those considered to be online for study purposes). The medium voltage (MV) distribution cables are represented by an equivalent impedance to reflect the aggregate impact of the collector system together with the substation step-up collector transformer(s). The total charging capacitance of the collector system should also be included as it can be significant with large size wind farms. A third option for wind farm modelling is to model several groups of WTGs, each represented by a single model, with a simplified representation of the collector system.

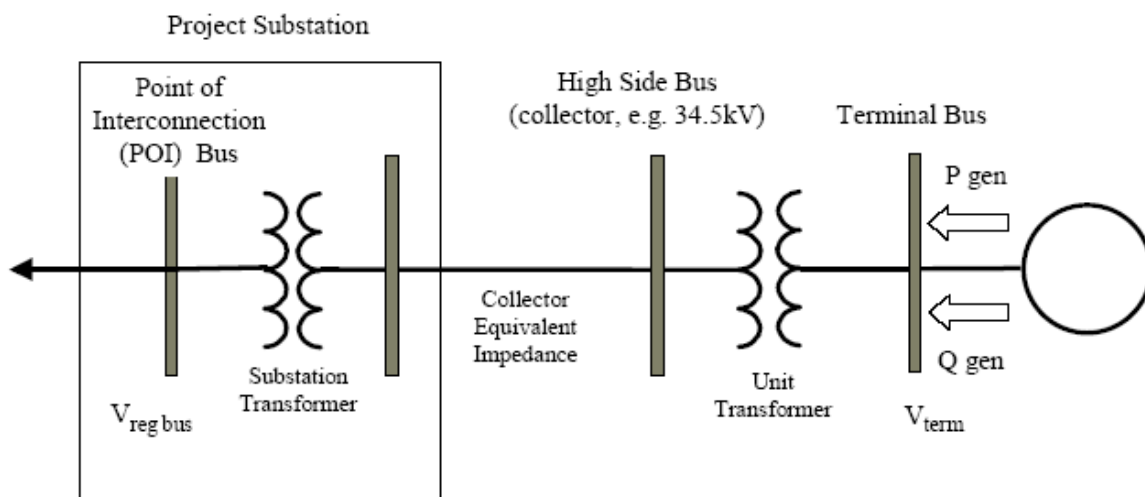


Figure 2-1. Wind turbine load flow model.

In this study, the assigned active and reactive power capabilities to the considered individual 6 MW WTG are listed in Table 2-1. The wind farm aggregate WTG is modelled as a conventional generator connected to a (PV) bus. Its active and reactive power capabilities (P_{max} , Q_{max} , and Q_{min}) are input as N times the capability of each individual 6 MW unit. The table shows also the nominal voltage at the WT generator terminals and the typical unit transformer rating and impedance. The distribution voltage level of the collector system is assumed to be 34.5 kV. The substation collector transformer is suitably rated for the number of WTGs.

Table 2-1. WTG load flow data

Generator rating	6.67 MVA
Generator active power	6 MW

Maximum generator reactive power	2.91 MVAR
Minimum generator reactive power	-2.91 MVAR
WTG terminal voltage at 50 Hz (V_{term})	4.16 kV
Unit transformer rating	6.67 MVA
Unit transformer Z	6 %
Unit transformer X/R	7.5

* Q_{max} and Q_{min} are such that the WTG is capable of producing 0.9 pf at the terminal (lagging and leading respectively)

2.2 Test System Parameters

The single line diagram of the test system considered in this study is shown in Figure 2-2. It represents an aggregate model of an offshore wind farm, which is adequate for most planning studies and would be suitable for analyzing the wind farm VAR control performance. GE's PSLF load flow and dynamic simulation software was used to model the wind farm and the associated electric grid connections.

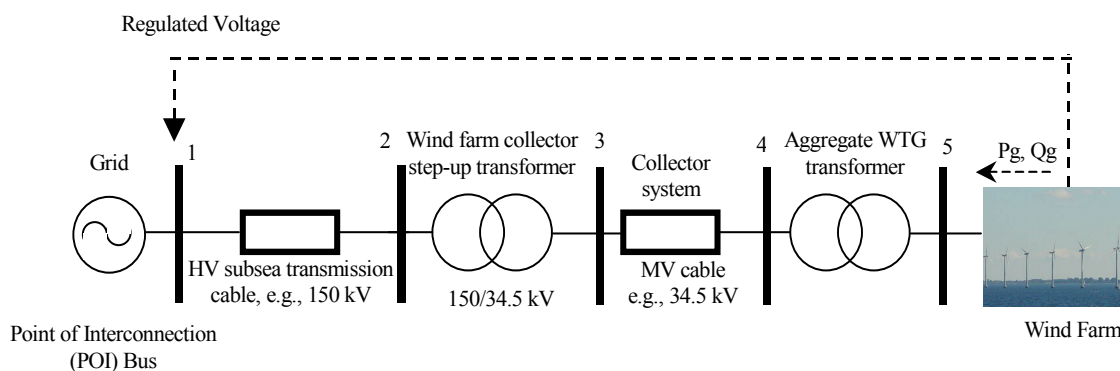


Figure 2-2. Test System.

The wind farm has a local grid collecting the output from the machines into a single point of connection to the grid (Bus 4). The system shown includes a single WTG model rated at 360 MVA (324 MW) to represent the aggregation of 54 WTGs each of 6 MW. The figure has also an aggregate WTG transformer and a 34.5 kV feeder representing the aggregate medium voltage collector system. A 360 MVA substation transformer is included to step-up the MV distribution system level to the high voltage (HV) system level, which is assumed to be at 150 kV (Bus 2). An equivalent impedance is used to represent the HV subsea transmission cables for power transmission to the shore. It is worth mentioning that the load flow is performed such that the wind farm WTG regulates the voltage at Bus 3 to 1.01 pu. Bus 1, where the HV transmission cables are connected to the electric grid, was chosen to be the point of interconnection (POI) with the capability to have voltage measurements. The wind farm VAR control structure is implemented to regulate the voltage at this bus during any grid disturbance. Bus 1 (grid) is an infinite bus. Generally, line drop compensation may be used to regulate the voltage at a point some distance from the voltage measurement bus.

Table 2-2 lists the system data with transmission distance of 30 km. Different grid short circuit ratios (SCRs) at the POI are considered, namely SCR 20, 5, and 3. This represents different strength levels of the grid ranging from a very strong system (SCR=20) to a relatively weak system (SCR=3). The SCR is calculated as the ratio of the short circuit MVA at the POI to the WTG MVA rating. All network impedances in the table are based on a 360 MVA base except the MV collector and HV transmission cable impedances are based on 100 MVA.

The selected MV and HV cable number and size are based on an investigation conducted for the wind farm design in Upwind WP9.

Table 2-3 summarizes the chosen configurations based on which the cable impedances were determined [3]. The cable resistances were calculated at 60 C°.

Table 2-2. Wind farm system data

Grid impedance for SCR 20, 5, and 3	X=5, 20, and 33 %
Load flow regulated voltage at bus 3	1.01 pu
Load flow POI voltage at bus 1	1.00 pu
Aggregate WTG transformer impedance	X=6% with X/R=7.5
Step-up collector transformer impedance	X=10% with X/R=10
Aggregate MV distribution feeder impedance (Z) and shunt susceptance (B)	Z=0.0032+j0.0079 pu B=0.1275 pu
Aggregate HV transmission cable impedance (Z) and shunt susceptance (B)	Z=0.0018+j0.0056 pu B=1.0815 pu

Table 2-3. MV and HV system cable configurations

Scheme	MV distribution cables	HV transmission cable
Voltage level (kV)	36	150
Cable size (mm ²)	500	500
Cable length (km)	10	30
Number of cables	11	3
Cable resistance (ohm/km)	0.0413	0.0413
Cable inductance (mH/km)	0.33	0.40
Cable capacitance (uF/km)	0.31	0.17

2.3 Impedance Allocation of Test System Components

In order to have an idea about the contribution of system components to the total impedance of the test system, the percentage impedance of each component of the total impedance was calculated. The calculation considered the impact of the system short circuit ratio (SCR) and the number of WTGs online. This obtained the impedance range of different system components. Accordingly, the proposed scheme for VAR control can be reasonably applied to any other system where the parameters lie within the range of those under study and similar system response would be anticipated.

Figure 2-3 and Figure 2-4 show the impedance in percent of the different system components with different SCRs with all and half of the WTGs online respectively. With half of the WTGs in service, only the associated MV collector feeders are considered to be energized according to the portion of connected WTGs. Not all collector feeders are connected for partial energization. This results in a higher equivalent feeder impedance. On the other side, all the HV transmission cables are connected irrespective of the number of connected WTGs. Table 2-4 lists the impedance range that can be extracted for each component. It shows that the equivalent WTG transformer and collector transformer as well as the grid impedances constitute the major parts of the total system impedance and should be carefully considered. The distance of the wind farm from the shore and therefore the length of the HV transmission cables has relatively little impact on the system impedance.

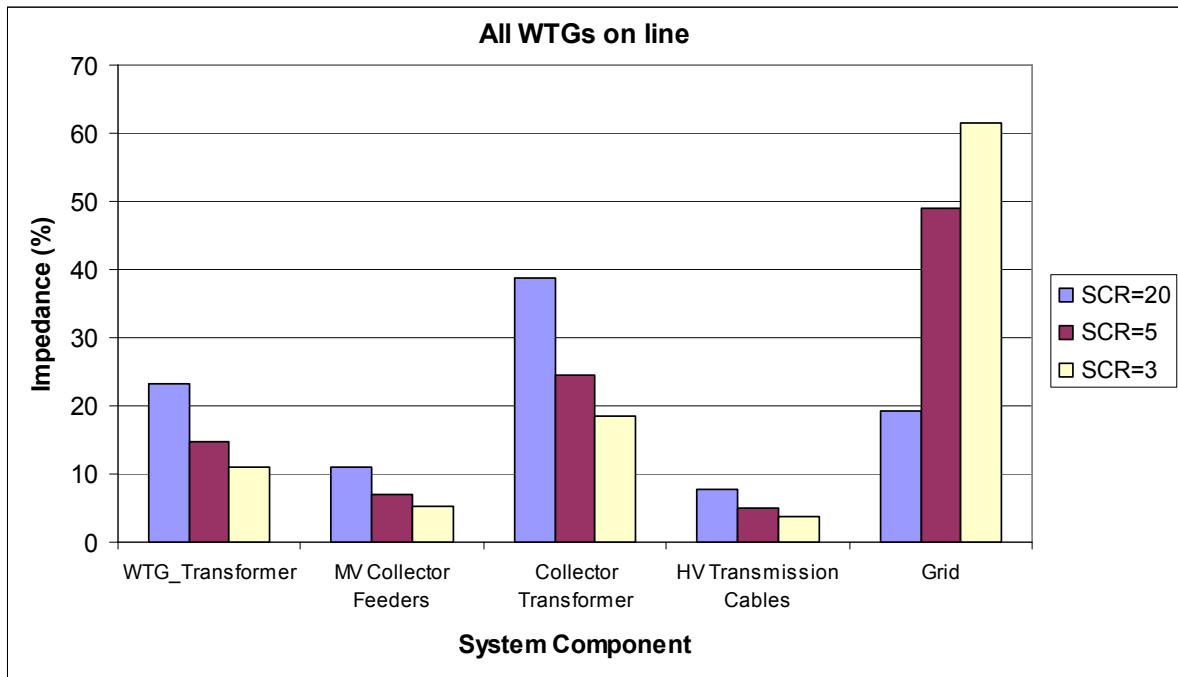


Figure 2-3. Impedance allocation of system components with all WTGs online.

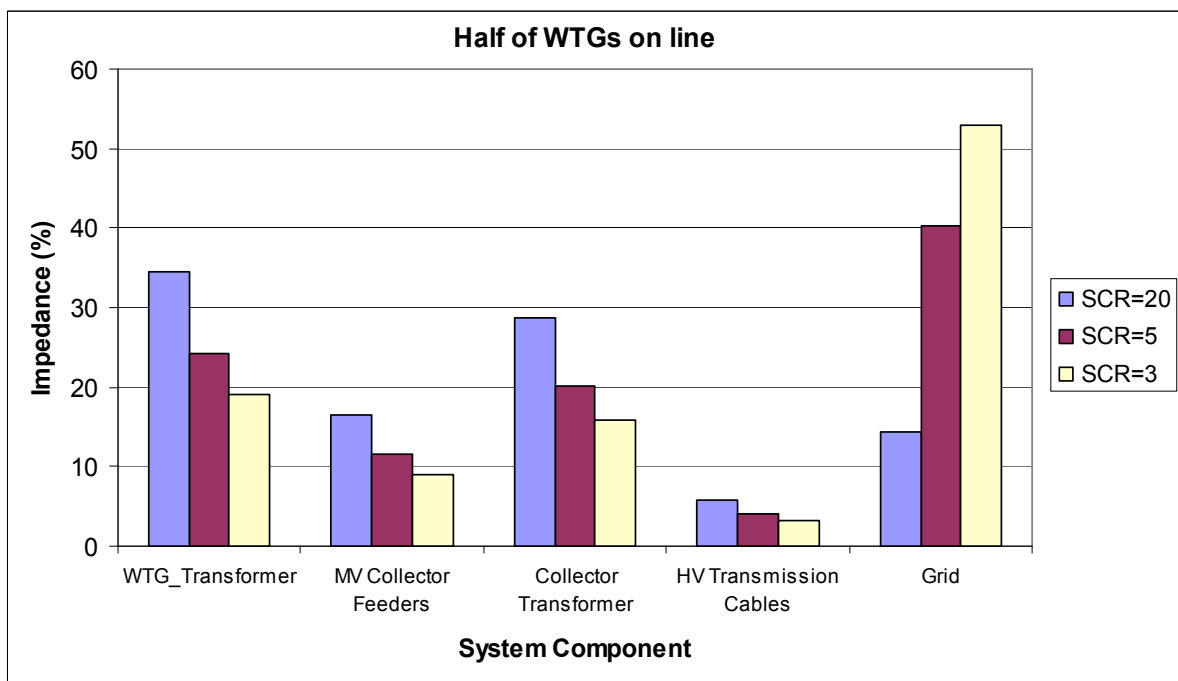


Figure 2-4. Impedance allocation of system components with half of WTGs online.

Table 2-4. Impedance contribution range of different components of the test system

System Component	Impedance range (%)
WTG Transformer	11-34
MV Collector feeders	5-16
Collector Transformer	16-39
HV transmission cable	3-8
Grid	14-62

3. Wind Farm VAR Control for WTGs with Power Electronics for Grid Interface

This section presents the design of a wind farm VAR control for wind turbines utilizing power electronics for the grid interface. The focus will be on doubly fed induction generator (DFIG) machines. Representation of the wind farm by one or two aggregate WTGs is performed. The electrical system described in Section 2 is considered for the design verification. Different scenarios of the number of connected wind turbines in the wind farm and different wind farm power levels are investigated to identify the main factors that have critical impact on the wind farm VAR control performance. This provides insight into the design procedure to be followed considering the variation of wind farm operating conditions and system parameters whilst maintaining the desired system voltage response.

3.1 Wind Farm VAR Design Guidelines

The wind farm VAR control block diagram is shown in Figure 3-1. The objective is to regulate the voltage at the point of interconnection “POI” (V_{reg}) according to a reference value (V_{reg_ref}). A WTG has an inner voltage control loop that regulates the WTG terminal voltage (V_{WTG}). In addition, there is a reactive power (or power factor) control loop that regulates the WTG reactive power output (Q_{gen}) (or power factor). The reactive power command (Q_{cmd}) can be a set point or can come from the supervisory VAR control. K_v is the WTG voltage loop integral gain and K_q is the WTG reactive power loop integral gain. The maximum and minimum aggregate WTG reactive power limits (Q_{max} and Q_{min}) are determined based on a turbine power factor rating of 0.9, which translates into reactive power limits of +/- 0.436 pu. K_p and K_i are the supervisory VAR control proportional and integral gains. The maximum and minimum WTG terminal voltage limits (V_{WTG_max} and V_{WTG_min}) are set to 1.1 and 0.9 pu respectively.

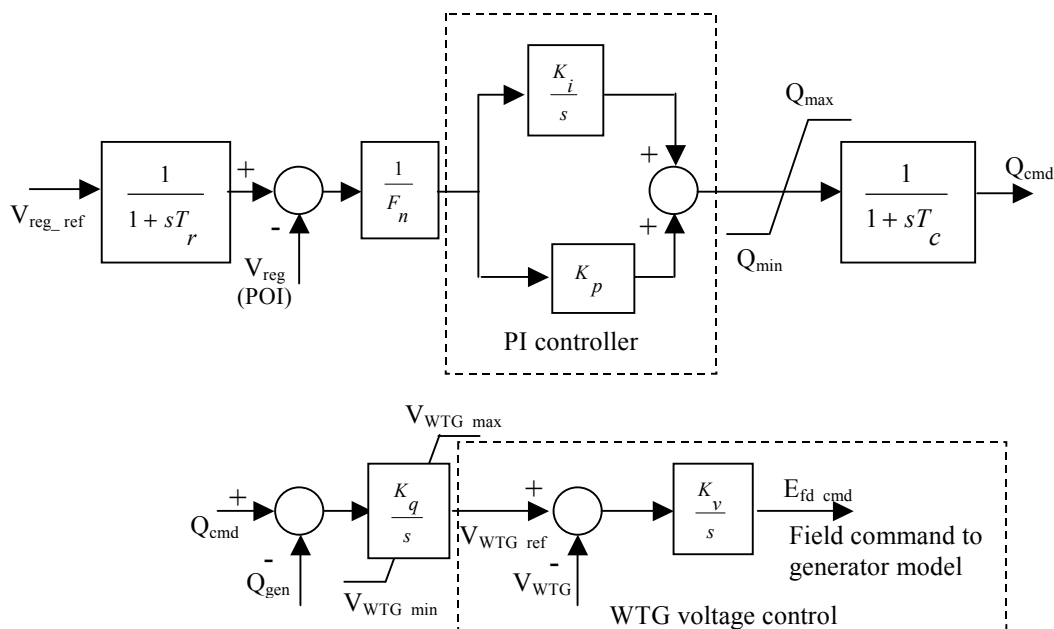


Figure 3-1. Wind farm VAR control block diagram.

The VAR control monitors the voltage at the POI and compares it against the reference voltage. The regulator itself is a PI controller. The output of the PI controller is the reactive power command (Q_{cmd}) sent to the WTGs. The time constant T_c reflects the delays associated with cycle time, communication delay to the individual WTGs, and additional filtering in the WTG controls. The voltage measurement lag is represented by the time constant T_r .

The parameter F_n is the fraction of wind turbines in the wind farm that are online. For example, if a case represents a condition with half of the wind turbines online, F_n should be set to 0.5. In this case the MVA base of the generator should also be set to one-half of its full value, and the MW capability of the turbine should be set to one-half of its full value. If a wind farm is represented by more than one WTG model, the F_n values of each should be set to the same value.

In order to have the desired response of the regulated voltage, the control parameters of different control loops should be properly selected. This section gives guidelines on tuning the parameters of different controllers.

3.1.1 WTG Voltage Control Loop

The WTG voltage control loop obtains the generator reference voltage (V_{WTG_ref}) from the reactive power controller and compares it against the WTG terminal voltage (V_{WTG}). The voltage error is multiplied by the gain K_v and integrated to compute the generator field voltage command. The parameter K_v in the integrator of the voltage control loop determines the time constant of WTG voltage control T_v . With DFIGs, the response of the converter is fast enough to neglect the dynamics, and therefore the WTG terminal voltage follows the command output of the integral K_v/s instantaneously (here s denotes the Laplace variable). The voltage loop dynamics are dominant, with the time constant T_v , which is usually in the range of milliseconds. Accordingly, a K_v value of 40 is reasonable to represent a time constant of 25 msec. Also, the WTG voltage loop dynamics apply only to the associated WTG and are independent from the number of individual WTGs in operation.

3.1.2 Reactive Power Control Loop

The time constant (T_q) of the reactive power demand response of the WTG without the wind farm VAR control is determined using the integral gain K_q . Considering the fact that the WTG voltage control loop response is much faster than that in the reactive power control loop, T_q can be determined as follows [4]:

$$T_q = \frac{X_{total}}{V_{WTG} \cdot K_q} \quad (3.1)$$

$$X_{total} = X_{WTG_tr} + X_{MV_feeder} + X_{collect_tr} + X_{HV_cable} + X_{grid} \quad (3.2)$$

The impedances are in pu based on the full size wind farm MVA where:

X_{total} : the impedance from the aggregate wind turbine generator terminals to the grid,

X_{WTG_tr} : the impedance of the aggregate WTG terminal transformer,

X_{MV_feeder} : the impedance of the aggregate MV collector feeder,

$X_{collect_tr}$: the impedance of the step up collector transformer,

X_{HV_cable} : the equivalent impedance of the HV subsea cables,

X_{grid} : the grid impedance representing the grid strength.

V_{WTG} : the WTG terminal voltage.

In other words, after determining the desired WTG reactive power control time constant for a specific system total impedance, the value of K_q can be calculated by:

$$K_q = \frac{X_{total}}{V_{WTG} \cdot T_q} \quad (3.3)$$

The previous equation neglects from the system impedance the resistive component and shunt capacitances. The value of T_q is in the order of seconds. It is clear that designing the VAR control depends on the total system pu impedance. Any variation of the grid strength level or the number of connected WTGs would affect the system basic time constant.

With a fraction F_n of WTGs online, X_{total} is calculated by:

$$X_{total} = X_{WTG_tr} + X_{MV_feeder} + F_n \cdot (X_{collect_tr} + X_{HV_cable} + X_{grid}) \quad (3.4)$$

Therefore, K_q should be adjusted if the change of X_{total} is significant with different number of WTGs online for the same system SCR in order to have a reasonable voltage response at the regulated bus. With 50% WTGs in the test system and with SCR of 20, X_{total} is almost 30% of that with all WTGs online. A lower value of K_q would be obtained with higher system SCR for the same reactive power control time constant.

3.1.3 Wind Farm VAR Control Loop

The VAR control loop includes the WTG voltage and reactive power control loops. As mentioned before, the WTG voltage control time response is fast, and thus the reactive power control integral gain plays a main role in the design of the VAR control (namely, the PI controller in Figure 3-1). The PI controller transfer function can be written as $\frac{K_i}{s} \left(1 + \frac{K_p}{K_i} s\right)$.

The ratio K_p/K_i is determined such that to cancel the effect of the reactive power control loop time constant T_q , i.e.,

$$\frac{K_p}{K_i} = T_q \quad (3.5)$$

Having the value K_p/K_i adjusted as in equation (3.5), the wind VAR control time constant can be obtained by [4]:

$$T_{var} = \frac{V_{POI}}{X_{grid} \cdot K_i} \quad (3.6)$$

It can be inferred that for the same VAR control time constant, the value of K_i would be higher with a stronger grid, i.e., with higher short circuit ratio.

With F_n representing the fraction of WTGs in the wind farm that are online, the factor $1/F_n$ is needed in the control loop to counteract the reduction of wind farm MVA base and the increase of equivalent pu WTG reactive power. This would recover the desired system control response. The F_n adjustment is possible when the number of connected WTGs “N” can be measured in the implementation of the wind VAR control.

3.2 Wind VAR Control Parameters Determination

From the aforementioned guidelines, the different wind VAR control parameters for the considered test system were determined and are listed in Table 3-1 for different grid short circuit ratios (SCRs). The wind farm VAR control time constant (T_{var}) was chosen as 3 seconds, and the reactive power control time constant (T_q) of the aggregate WTG without the VAR control was chosen as 0.5 seconds. It is worth mentioning that the parameters were determined assuming that all individual WTGs are online. With a fraction of the WTGs online, the control parameters might be recalculated if the variation of the total system per unit impedance X_{total} is significant.

Table 3-1 VAR Control Parameters with DFIG machine for Different SCRs

SCR	T_{var} (sec)	T_q (sec)	K_q	K_p	K_i
20	3	0.5	0.5	3.33	6.66
5	3	0.5	0.82	0.833	1.66
3	3	0.5	1.08	0.5	1.0

3.2.1 Response to a WTG Step Reactive Power Command

This section examines the WTG response to a step reactive power command (Q_{cmd}). The amount of WTG reactive power (Q_g) required to change the voltage at the POI is inversely proportional to the total system impedance. In other words, for the same WTG reactive power command change, the POI voltage variation would be lower for stronger systems. If the WTG is directly connected to the POI bus with a system short circuit ratio of 20, a 20% Q_g change is needed for 1% voltage variation at the POI, whereas a 3% Q_g change is needed with a short circuit ratio of 3.

Figure 3-2 shows the WTG generated reactive power response as well as the response of both the WTG terminal voltage (blue line with o marks) and the regulated voltage at the POI (red line with x marks). The minimum and maximum value of the y-axis are shown below the x-axis as indicated in the lowest plot. The magnitude of the step reactive power command is lower with lower short circuit ratio so that the WTG terminal voltage does not exceed its maximum limit.

The step reactive power increase was set to 0.3, 0.15, and 0.1 pu for SCRs 20, 5, and 3 respectively. It can be seen that the time needed by the WTG to provide the required reactive power command complies with the designed value of T_q . This was achieved with different SCRs due to the adaptation of the K_q value for each grid strength level.

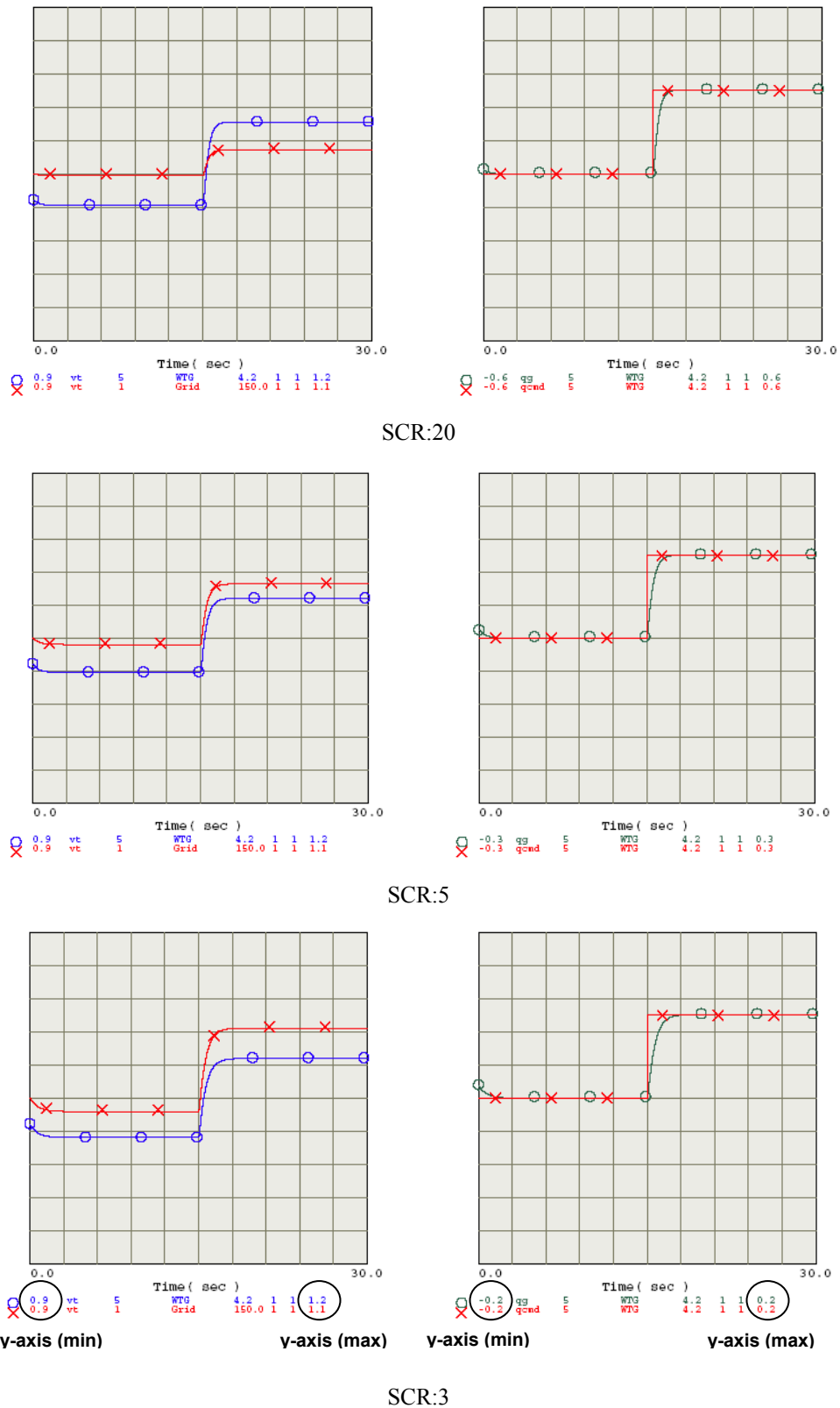


Figure 3-2. System response to a step reactive power command (Q_{cmd}) for different SCRs.

3.2.2 Response to a Step Change of Regulated Voltage

The WTG response to a step change of regulated voltage command at the POI was examined. Different wind farm power levels and different numbers of connected WTGs were investigated. The control parameters listed in Table 3-1 were used.

All WTGs are Connected at Full Load (324 MW, $F_n=1$)

With all WTGs connected at full load, the regulated voltage step change was set to 0.015 pu for different system SCRs. Figure 3-3 shows the response of the POI voltage and WTG reactive power with $F_n=1$. It is clear that the voltage at the POI is smoothly increasing to its new set value according to the designed time constant of the VAR control. This is noticed for different system SCRs with appropriate settings.

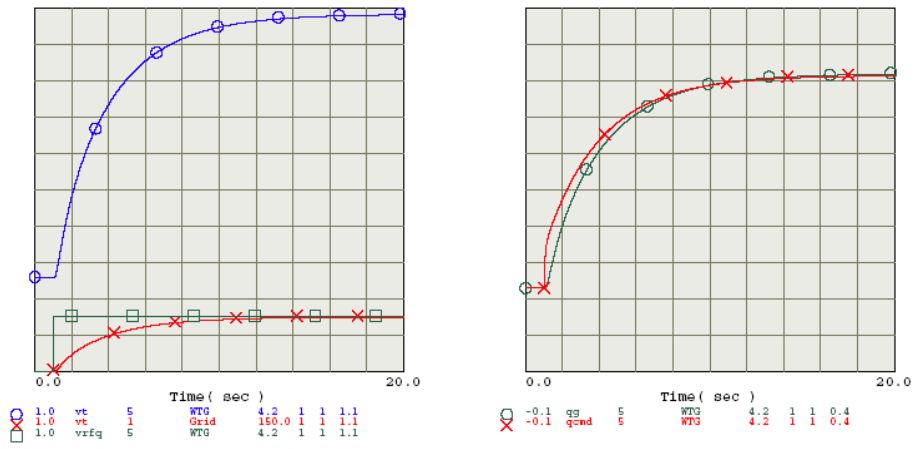
Half of the WTGs are Connected at Full Load with (162 MW, $F_n=1$)

With half of the WTGs connected at full load, the amount of WTG reactive power change required for the same step of voltage magnitude will be double of that when all WTGs are connected (inversely proportional to the portion of the WTGs in service). This can cause the WTG terminal voltage to hit the maximum voltage limit and the new reference value of the regulated voltage at the POI would not be achieved. This is likely to happen especially with higher system SCR. Therefore, the step voltage change in this case was reduced to 0.01 pu. The value of F_n was kept equal to 1, i.e., the wind VAR performance dependence on the number of WTGs in service was not considered.

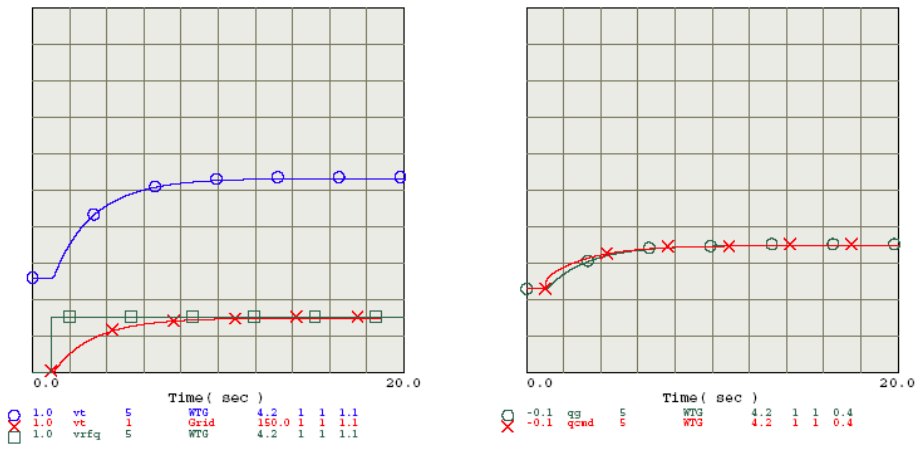
Figure 3-4 depicts how the POI voltage response in terms of the settling time became slower because the information about the number of connected WTGs was not taken into account. When double the pu WTG reactive power change is required, more time will be needed. Therefore, the factor F_n should be set to 0.5, so that the VAR control loop gain is doubled and consequently, the wind VAR control time constant is back to the original designed value when all WTGs are in service.

Half of the WTGs are Connected at Full Load (162 MW, $F_n=0.5$)

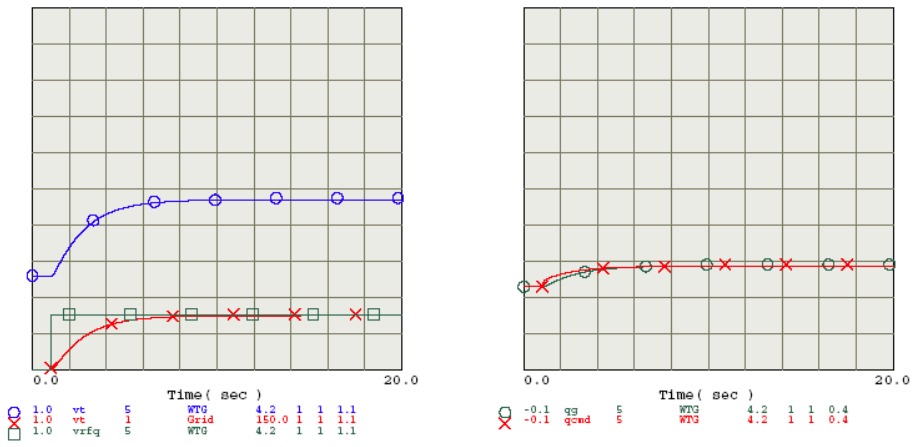
Figure 3-5 shows the response of the previous case to a step change of regulated voltage of 0.01 pu with the factor F_n set to 0.5. The response depicts how this could help recover the desired wind VAR response for different system SCRs where the POI increased smoothly as required to the new regulated value.



SCR:20

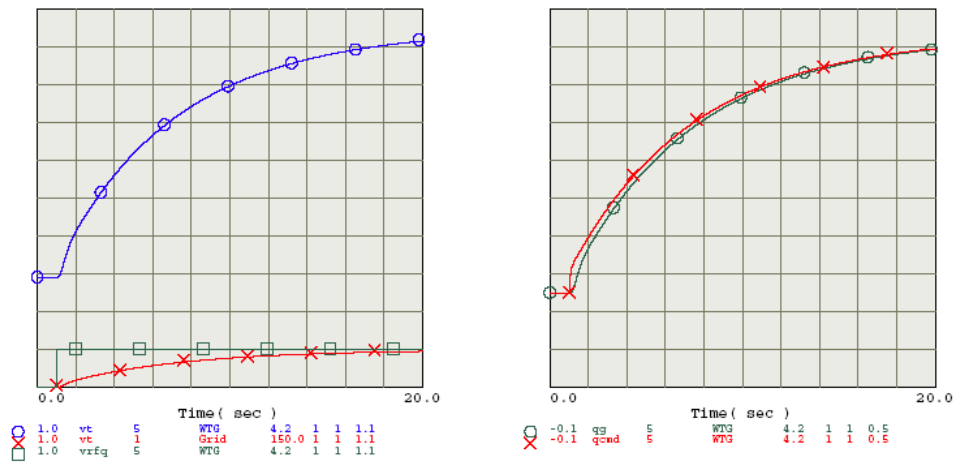


SCR:5

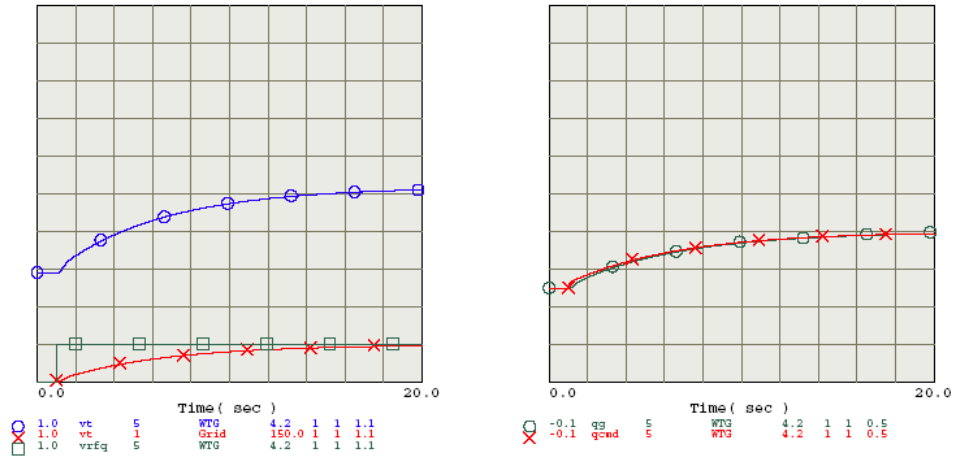


SCR:3

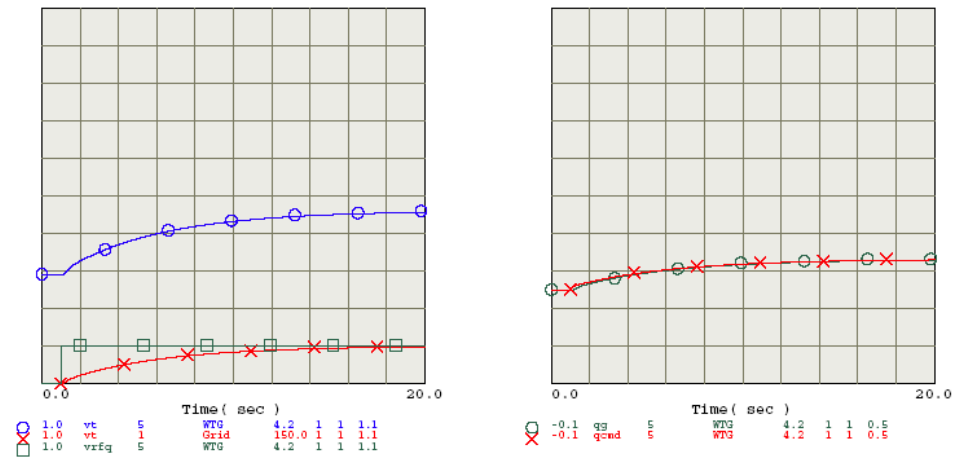
Figure 3-3. System response to a step change of regulated voltage for different SCRs (324 MW, all WTGs are connected at full power).



SCR:20

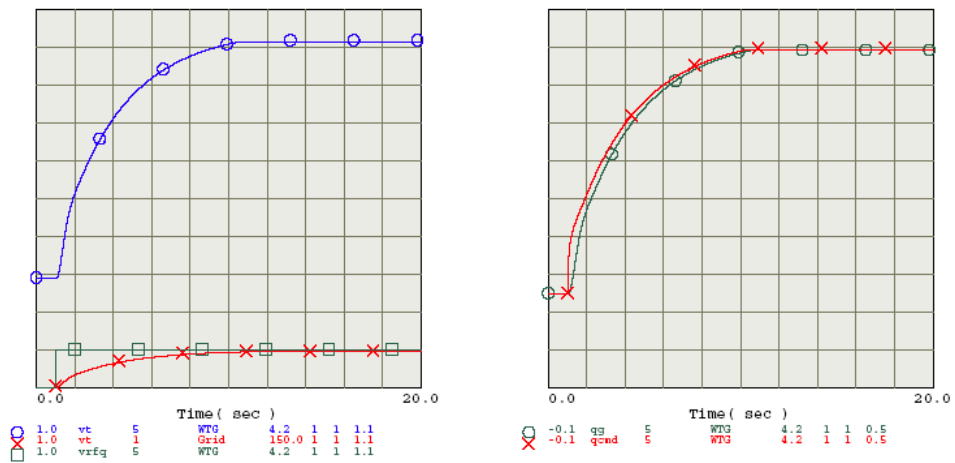


SCR:5

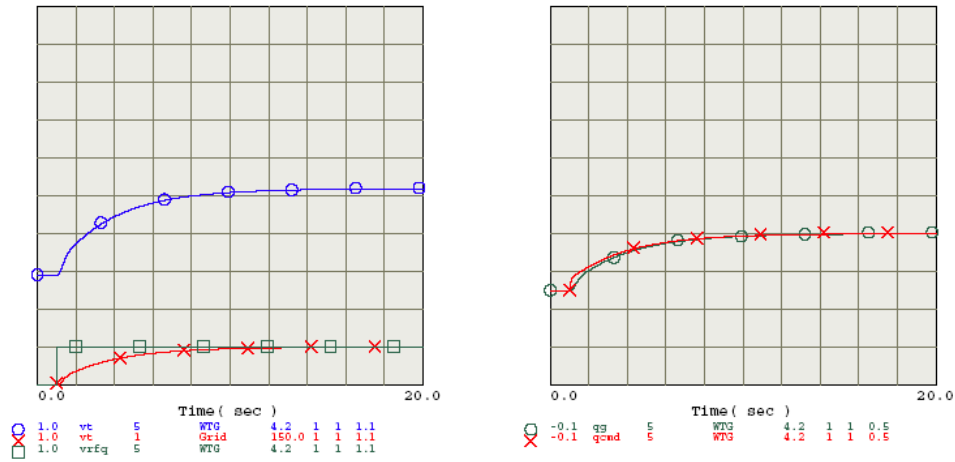


SCR:3

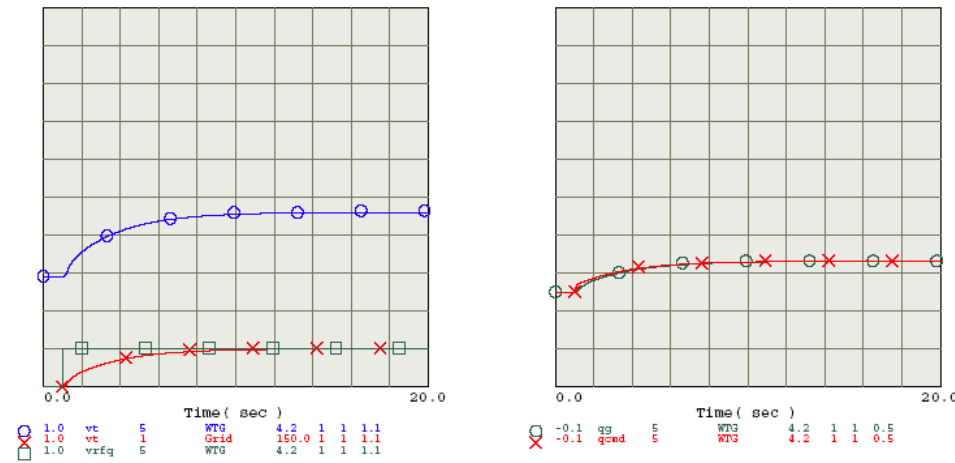
Figure 3-4. System response to a step change of regulated voltage for different SCRs with $F_n=1.0$ (162 MW, half of WTGs are connected at full power).



SCR:20



SCR:5



SCR:3

Figure 3-5. System response to a step change of regulated voltage for different SCRs with $F_n=0.5$ (162MW, half of WTGs are connected at full power).

3.3 Simulation Results with One and Two Aggregate WTGs Model with DFIG

In this section, the wind farm VAR control performance is presented with the wind farm model utilizing one or two aggregate WTGs with doubly fed induction machines. The supervisory VAR control implementation with two aggregate WTGs was performed using a user model written in the GE PSLF software program. Figure 3-6 shows the supervisory control structure and wind farm representation. The VAR control functions to regulate the voltage at the POI by calculating the required total reactive power from the wind farm generators. Then, it allocates a reactive power command to each aggregated WTG according to the respective MVA base, i.e., the number of individual WTGs in service in each aggregate model.

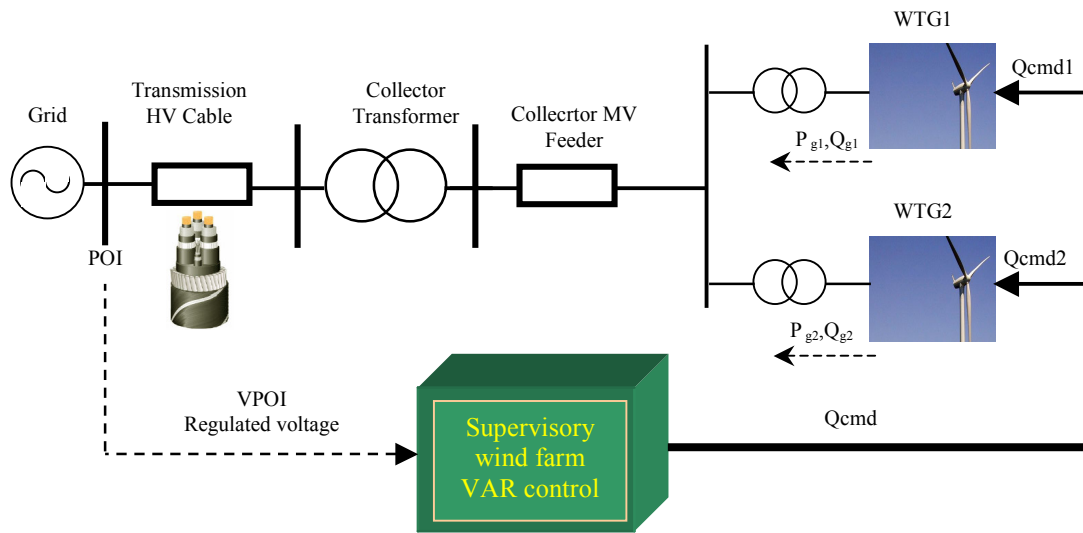


Figure 3-6. Wind farm representation and the VAR control structure.

3.3.1 Test Cases

The control performance was investigated by applying a capacitive impedance load at the POI bus. This raises the associated voltage and accordingly the supervisory VAR control reacts to bring the POI voltage back to the initial value. Different scenarios were considered and can be summarized as follows:

- Scenario 1: Two aggregate WTGs each at full power with all individual WTGs in service,
- Scenario 2: Two aggregate WTGs, one is at full power and the other one is at half power. Both have all WTGs in service,
- Scenario 3: Two aggregate WTGs, one is at full power with all WTGs in service and the other one is at half power with half of the WTGs are in service, $F_n=1$,
- Scenario 4: One aggregate WTG at full power with all WTGs in service, $F_n=1$,
- Scenario 5: One aggregate WTG at half power with all WTGs in service, $F_n=1$
- Scenario 6: One aggregate WTG at half power with half of the WTGs in service, $F_n=1.0$,
- Scenario 7: The same as scenario 6, but with F_n set equal to 0.5
- Scenario 8: Additional cases were simulated to investigate the implementation of the control settings of system SCR 20 to system SCRs 5 and 3 and implementing control settings of system SCR 3 to system SCR 20. A full power wind farm was assumed with all WTGs in service,
- Scenario 9: The effect of the initial WTG terminal voltage on the wind VAR performance was also explored for a system SCR of 20 with a half power wind farm with all WTGs in service.

The mentioned scenarios were simulated with different system SCRs 20, 5, and 3. The capacitive load was chosen for the different system SCRs to cause a similar step voltage magnitude change. The load capacitive impedances were 0.5, 2, and 3.5 pu, based on an arbitrary 100 MVA system, for system SCRs of 20, 5, and 3 respectively. More load injected capacitive reactive power is required with higher system SCR to have similar voltage step fluctuations.

3.3.2 Results Summary and Conclusions

The test cases and results are summarized in Table 3-2. The MVA base with two aggregate WTGs indicates if each one has all respective WTGs (180 MVA) or half of them (90 MVA) in service. The initial WTG reactive power gives an indication about the available reactive power margin to regulate the POI voltage. The settling time shows the VAR control performance and if the settings were appropriately tuned. It is the time taken to have the POI voltage settled within

+/- 10% of the steady state value. The control settings listed in Table 3-1 were applied unless otherwise stated for the additional special cases.

The following conclusions can be drawn from the results of the test cases listed in Table 3-2:

- Scenario 1: Having all individual WTGs in service resulted in acceptable VAR control response. The available WTG reactive power margin was high enough to absorb reactive power and compensate for the inserted capacitive load. This is due to two reasons, firstly the availability of all WTGs and the associated higher reactive power capability; and secondly when the WTGs are operating at full load, they are over excited (producing reactive power) to regulate the steady state voltage at Bus 3 to 1.01 pu.
- Scenario 2: Having one aggregated WTG at full power and the other one at half power where all WTGs are in service would also have an acceptable response (settling time). The slight difference is that the WTGs are underexcited and absorb reactive power. This would reduce the reactive power margin required for voltage regulation. With system SCR 20, the WTG reactive power capability was just exceeded and the POI voltage settles at a value slightly higher than the desired steady state voltage at the POI.
- Scenario 3: One of the wind farm aggregate WTGs is at full power with all individual WTGs in service and the other aggregate WTG is at half power with half of the individual WTGs in service. The initial WTGs terminal voltage and total wind farm produced reactive power are almost the same as those in cases 1-3 in Table 3-2. The difference in this scenario (cases 7-9) is the lower reactive power capability of the second aggregate WTG and the larger requirement for reactive power in pu terms, due to the lower number of connected wind turbine units. This would slightly increase the settling time for system SCRs 5 and 3. For system SCR 20, the required reactive power was higher than the plant capability, and the POI voltage could not reach the desired steady state value.
- Scenario 4: One aggregated WTG is at full power with all individual WTGs in service. Results close to those in cases 1-3 were obtained with the same conclusions. Again the POI voltage just reached the steady state value and the WTG reaches its reactive power capability.
- Scenario 5: One aggregated WTG is at half power with all individual WTGs in service. The desired performance was achieved with results close to those in cases 4-6 (2 WTGs) and in cases 10-12 (1 WTG).
- Scenario 6: One aggregated WTG is at half power with half of the individual WTGs in service. A stable response was obtained, but is slow with a settling time that is larger than that when all WTGs are in service. With system SCR 20, the POI voltage did not reach the desired value because the required WTG reactive power was higher than the capability.
- Scenario 7: The same as scenario 6, but with the adjustment of the factor F_n to 0.5. A reasonable response was obtained with a settling time that is almost half of that obtained in scenario 6 for system SCRs 3 and 5 and is comparable to that obtained when all WTGs are in operation (scenarios 4 and 5). Adapting F_n according to the number of WTGs was demonstrated to maintain the desired time response by adjusting to the higher pu WTG reactive power variation requirement.
- Scenario 8: When the control settings for system SCR 20 were used for system SCRs of 5 and 3, the settling time was much faster. This is mainly because the VAR control time constant was modified due to firstly a higher value of grid impedance that increases total system impedance, and secondly having a higher K_i value determined with SCR 20. Therefore, the response speed would almost increase in proportion the square of the ratio of K_i value determined for the lower SCR (5 or 3) and the higher SCR (20). Hence, the settling time was noticeably reduced (cases 22 and 23). When the control settings for

system SCR 3 were applied for system SCR 20, the opposite occurred (case 24). The time response was much slower and the settling time was considerably increased.

- Scenario 9: The same as case 13 (SCR 20), but with higher WTG initial voltage. This was achieved by increasing the load flow controlled voltage at Bus 3 from 1.01 to 1.025 pu. Accordingly, the WTG was further overexcited to provide more reactive power. Consequently, the initial WTG terminal voltage was raised to 1.043 pu compared to 1.017 pu. This provided more reactive power margin to regulate the POI voltage with a reasonable performance without exceeding the WTG capability.

Table 3-2. Summary results of considered test cases for DFIG WTG

Scenario	Case	SCR	MVA base WTG1 (MW)	MVA base WTG2 (MW)	Wind farm power (MW)	Initial WTG1 Q (MVAR)	Initial WTG2 Q (MVAR)	Initial WTG1 V (pu)	Initial WTG2 V (pu)	Settling time (sec) *	Notes
1	1	20	180	180	324	2.617	2.617	1.026	1.026	5.3	
1	2	5	180	180	324	2.617	2.617	1.026	1.026	5.7	
1	3	3	180	180	324	2.617	2.617	1.026	1.026	5	
2	4	20	180	180	324	-0.138	-0.137	1.025	1.018	999	
2	5	5	180	180	324	-0.137	-0.138	1.025	1.018	6.1	
2	6	3	180	180	324	-0.14	-0.14	1.025	1.018	5.7	
3	7	20	180	90	243	3.991	1.995	1.027	1.027	999	
3	8	5	180	90	243	3.991	1.995	1.027	1.027	8	
3	9	3	180	90	243	3.991	1.996	1.027	1.027	7.4	
4	10	20	360	N/A	324	5.261	0	1.026	0	5.4	
4	11	5	360	N/A	324	5.261	0	1.026	0	5.8	
4	12	3	360	N/A	324	5.26	0	1.026	0	5.1	
5	13	20	360	N/A	162	-3.743	0	1.017	0	999	
5	14	5	360	N/A	162	-3.743	0	1.017	0	6.4	
5	15	3	360	N/A	162	-3.743	0	1.017	0	6.4	
6	16	20	180	N/A	162	8.851	0	1.029	0	999	F _n =1
6	17	5	180	N/A	162	8.851	0	1.029	0	12.2	
6	18	3	180	N/A	162	8.851	0	1.029	0	11.7	
7	19	20	180	N/A	162	8.851	0	1.029	0	999	F _n =0.5
7	20	5	180	N/A	162	8.851	0	1.029	0	6.3	
7	21	3	180	N/A	162	8.851	0	1.029	0	6.2	
8	22	3	360	N/A	324	5.261	0	1.026	0	1.8	Settings of SCR 20 were applied to SCR 3
8	23	5	360	N/A	324	5.26	0	1.026	0	1.4	Settings of SCR 20 were applied to SCR 5
8	24	20	360	N/A	324	5.261	0	1.026	0	999	Settings of SCR 3 were applied to SCR 20
9	25	20	360	N/A	162	41.945	0	1.043	0	6	Higher initial WTG terminal voltage

*Settling time of 999 sec indicates inability of the POI voltage to recover back to the steady state value

4. WTG Synchronous Machine

In this section, the wind turbine generator is modelled as a conventional synchronous generator directly connected to the grid, i.e., without power electronics interface as used with the DFIG machine. Regulation of the voltage at the point of interconnection is performed via the wind farm VAR control which provides a reference value of the WTG terminal voltage to the generator excitation system to obtain the desired POI voltage. The system dynamics is governed by the synchronous generator and its excitation system. Two different excitation system types were investigated; 1) Static excitation system; 2) Brushless excitation system. The field voltage of both types is affected by the generator terminal voltage that supplies the excitation system.

4.1 Static-Type Excitation System

All components in the static-type excitation system are stationary. The excitation system provides the synchronous generator DC field current by a thyristor bridge through slip rings. The supply of power to the thyristor bridge is from the terminals of the main generator via a step down transformer. Hence, the exciter output voltage is dependent on the generator AC voltage and, therefore, is affected by grid events and voltage variations. This excitation system has a relatively small time constant. The synchronous generator DC field is regulated in a closed loop configuration designed to maintain adequate field strength to control the generator terminal voltage.

4.1.1 Performance of Static-Type Excitation System

The block diagram of the excitation control system is shown in Figure 4-1. The exciter reference voltage (V_{WTG_ref}) is adjusted to regulate the WTG terminal (V_{WTG}). The difference between the generator terminal voltage and reference voltage is fed through a lead-lag controller and a gain block (K_e). The magnitude of K_e is calculated to maintain the voltage at full load and no load within 1% of each other [5]. The excitation voltages E_{max} and E_{min} are the field voltage output (E_{fd}) limits in pu. The generator is represented by its D-axis transient rotor time constant (T'_{do}). The parameters of the WTG excitation system were tuned to have a reasonable first order time response of the generator terminal voltage to facilitate the VAR control design. The control parameters are listed in Table 4-1 [6].

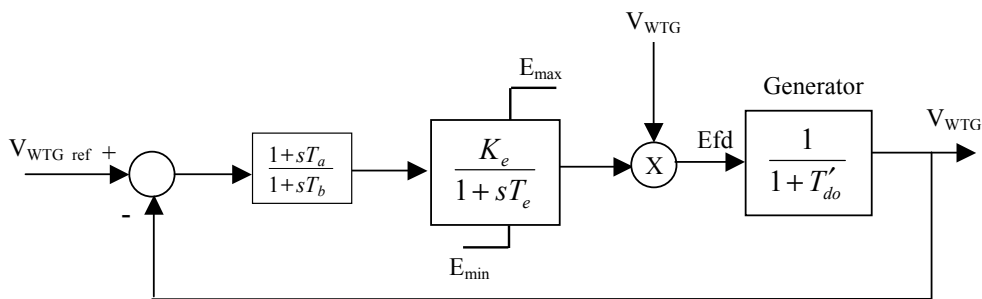


Figure 4-1. Static excitation control block diagram.

Table 4-1. Parameters of the control block diagram of the static excitation system

Parameter	Description	Value
T_a	Nominator time constant of lead-lag block (sec)	3
T_b	Denominator time constant of lead-lag block (sec)	30
K_e	Gain	200
T_e	Time constant of gain block (sec)	0.02
T'_{do}	Direct axis transient generator time constant (sec)	6.5

One of the common methods for evaluating generator performance and voltage stability is to calculate the frequency response of the excitation system with the generator. This gives the relationship in terms of gain and phase between the steady state sinusoidal inputs and the resultant steady-state sinusoidal outputs. The frequency response can be represented by Bode plots to compare the gain and phase angle of the excitation system transfer function versus frequency.

The open loop frequency response of the static excitation system shown in Figure 4-1 with the parameters listed in Table 4-1 is shown in Figure 4-2. It shows high stability of the system with fast response in terms of infinite gain and 83.8° phase margin. The cross over frequency at 0dB gain is 3.08 rad/sec.

The closed loop Bode plot is shown in Figure 4-3. The -3 dB point representing the bandwidth of the excitation system is at a frequency of 3.4 rad/sec. The gain remains very flat before it begins to roll off. This flat response indicates a very stable system with no voltage overshoot, which satisfies the IEEE Std. 421.2-1990 for guidance towards the evaluation of dynamic response of excitation control systems [7].

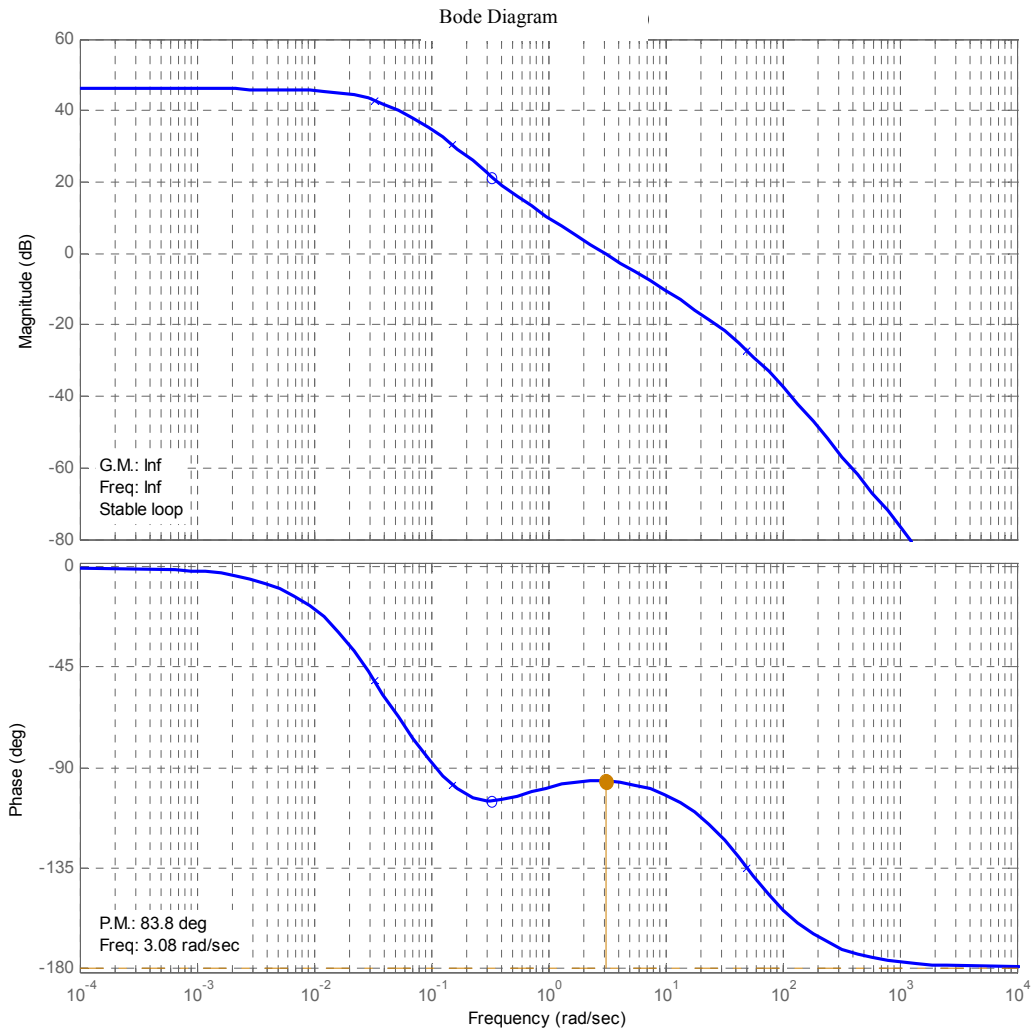


Figure 4-2. Open loop Bode diagram of the static excitation system.

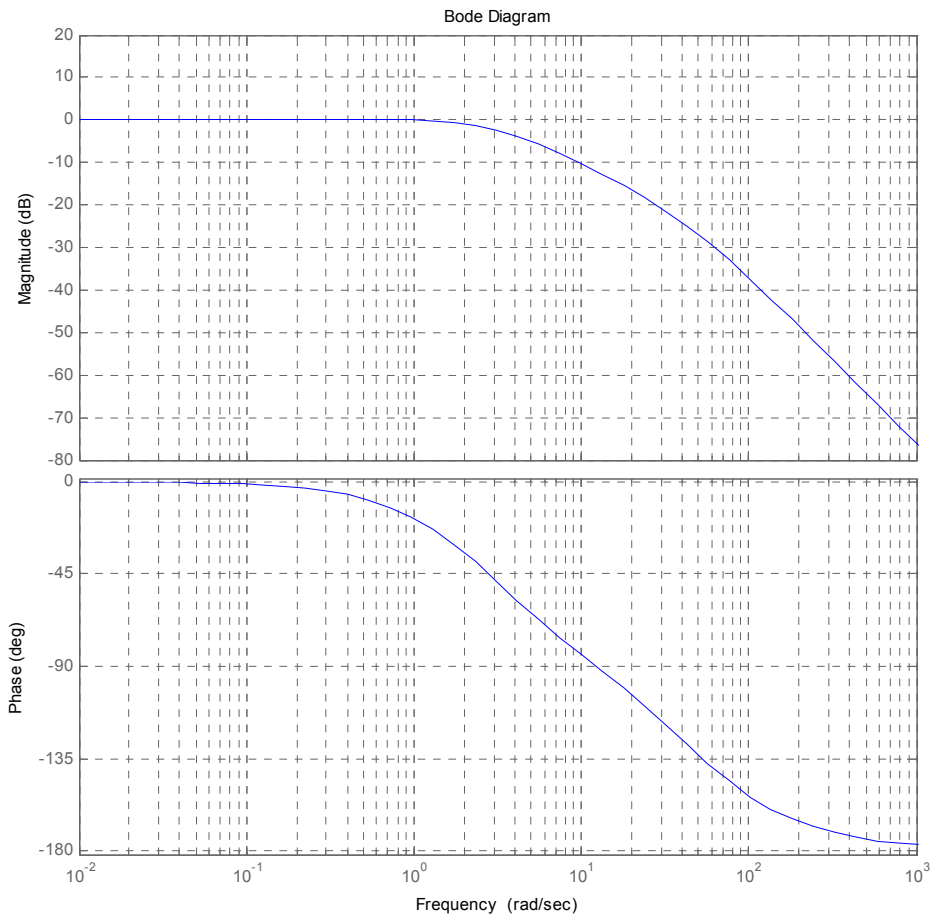
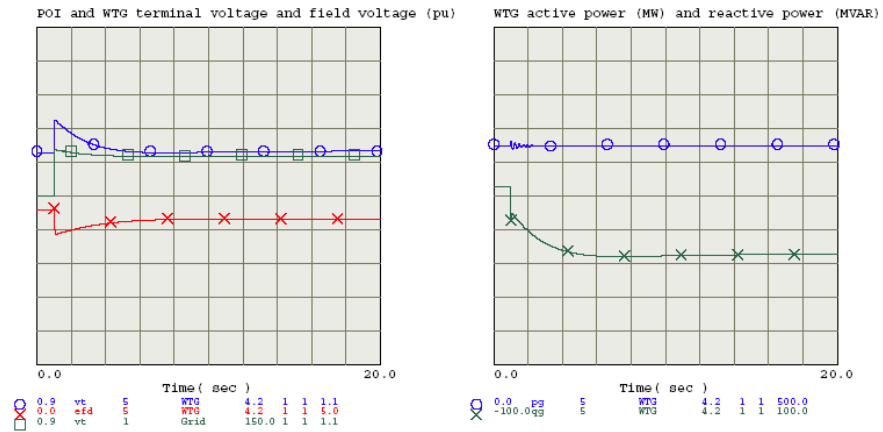


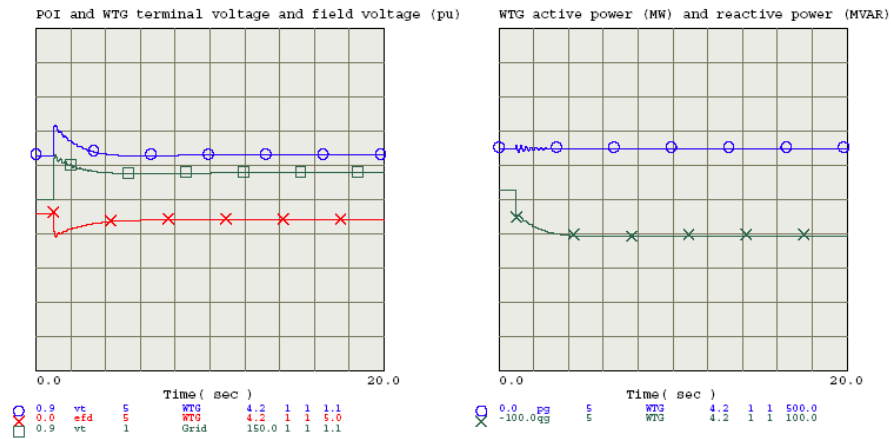
Figure 4-3. Closed loop Bode diagram of the static excitation system.

The excitation system performance was examined by switching a capacitive load impedance at the POI at Bus 1 of the considered test system in this report. This was performed with different system SCRs. The capacitive impedances were 0.5, 2 and 3.5 pu based on an arbitrary 100 MVA base with system SCRs of 20, 5, and 3 respectively to have almost the same step voltage change at the POI, and at the same time having the excitation system operating within the limits of its field voltage. Two different cases of wind farm power levels were considered. The first one was full power with all WTGs in service, and the second one was half power with half of the WTGs in service. The system response is shown in Figure 4-4 for full power and in Figure 4-5 for the half power case. The left plots depict the WTG terminal voltage (blue line) and field voltage (red line) as well as the POI voltage (green line). The right plots show the WTG active (blue line) and reactive power (red line).

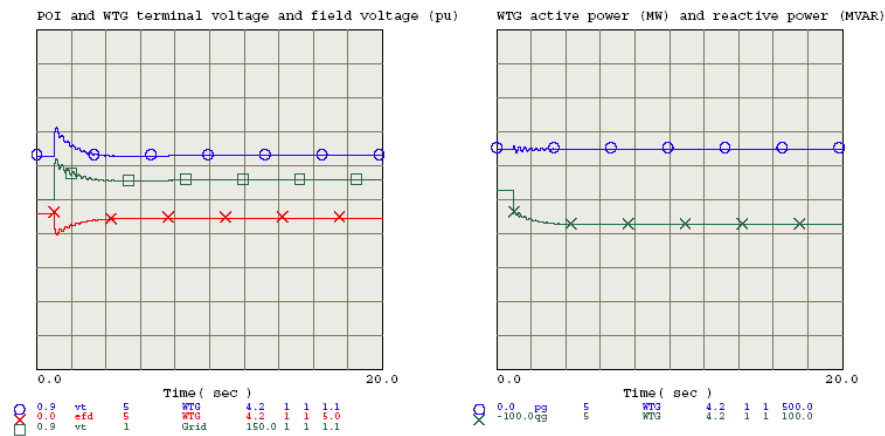
It can be inferred how the excitation system could provide a smooth response in regulating the WTG terminal voltage with a rough time constant of 2 seconds for system SCR of 20 and about 1 second for systems SCRs of 5 and 3. With half of the WTGs in service, the excitation time response is a little bit longer than that in the case with all WTGs in service. However, the difference is not noticeable. This shows that the system SCR has a more pronounced impact on the excitation system than that due to the number of connected WTGs.



SCR:20

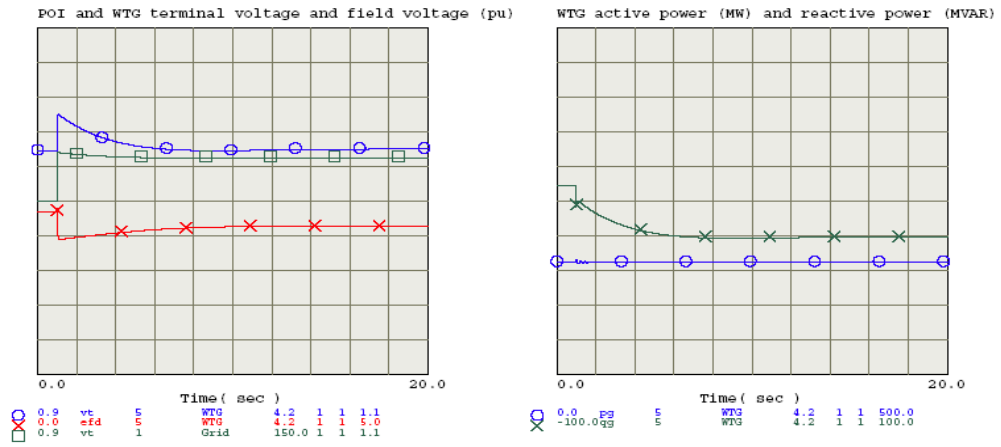


SCR:5

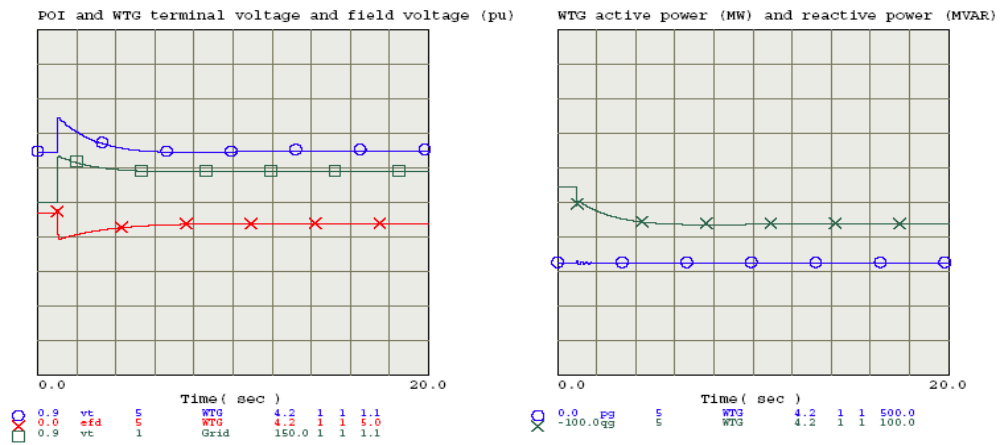


SCR:3

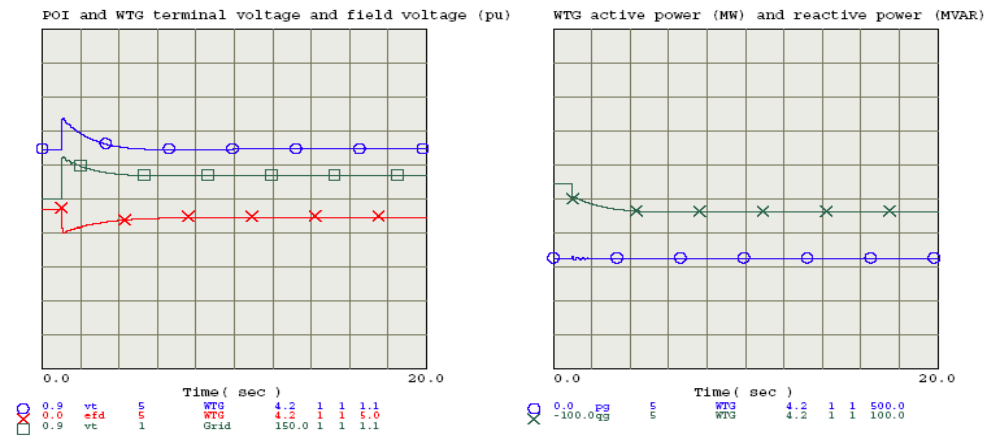
Figure 4-4. Static excitation system response with all WTGs in service (324 MW).



SCR:20



SCR:5



SCR:3

Figure 4-5. Static excitation system response with half of the WTGs in service (162 MW).

4.1.2 Wind Farm VAR Control using WTG Voltage Control

This section presents the design of wind farm VAR control with synchronous WTG with static-type excitation to regulate the POI voltage. The system control block diagram is depicted in Figure 4-6. The difference between the regulated voltage (V_{reg}) at the POI and the reference (V_{reg_ref}) value is regulated through a PI controller. The output of the PI controller (with anti-windup limits) provides the WTG reference voltage (V_{WTG_ref}) to the excitation system to obtain the necessary field voltage (E_{fd}). The factor F_{sc} is used to derive the regulated voltage at the POI from the WTG terminal voltage (V_{WTG}). The value of F_{sc} is approximately equal to the ratio between the impedance seen from the POI bus to the system infinite bus (X_{grid}) to the total system impedance (X_{total}). This ratio can be set up in the VAR control implementation. It can be inferred that the value of F_{sc} depends on the grid SCR and the number of connected wind turbines. With the lead-lag controller and a relatively high value of the gain K_e , there will be a small difference between the V_{WTG_ref} and V_{WTG} . Table 4-2 shows how F_{sc} varies with the number of WTGs connected in the test system. With 50% of system WTGs online, the variation of F_{sc} is not significant and not expected to have a noticeable impact on the system performance. The VAR control described here is implemented using the GE PSLF software in a written user model.

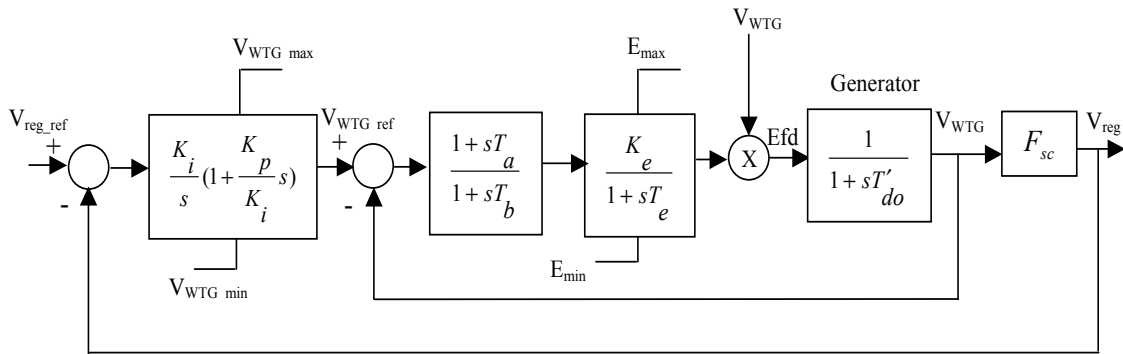


Figure 4-6. Wind farm VAR control block diagram with static excitation system.

Table 4-2. Variation of F_{sc} value for different system SCRs with different number of WTGs

SCR	20	5	3
F_{sc} (all WTGs connected)	0.2	0.49	0.62
F_{sc} (half of WTGs connected)	0.144	0.4	0.53

4.1.3 Tuning the PI Controller

The PI controller design is based on the same criteria that has been followed with the VAR control for the DFIG machine. The value of K_p/K_i is set to cancel the time constant of the excitation system. The value of K_i is selected according to the desired VAR control time constant (T_{var}) while compensating for the value of F_{sc} according to the following equation:

$$K_i = \frac{1}{T_{var} F_{sc}} \tag{5.1}$$

The VAR control time constant was set to 3 seconds. The chosen values of K_p and K_i with all WTGs in service are listed in Table 4-3.

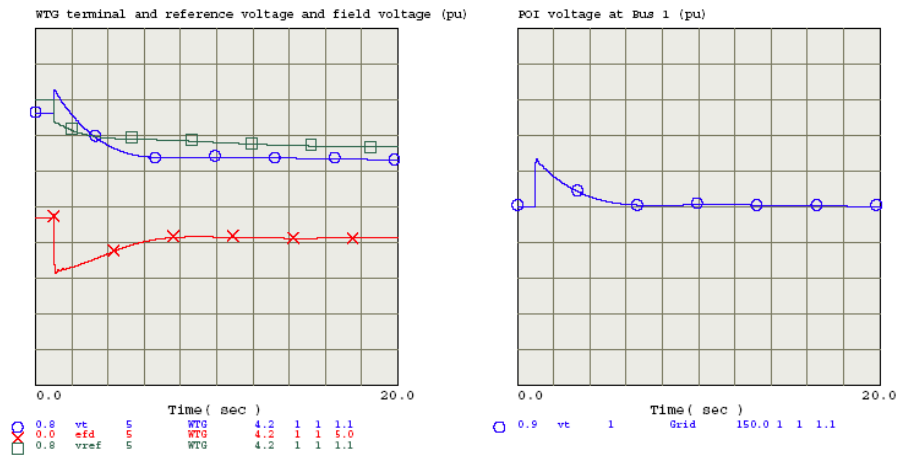
Table 4-3. VAR control parameters with static excitation system

SCR	T_{var} (sec)	F_{sc}	K_i	K_p
-----	-----------------	----------	-------	-------

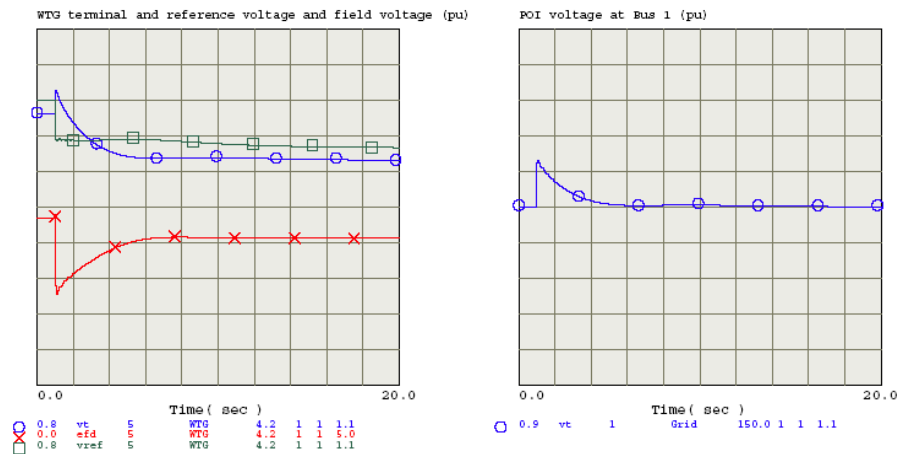
20	3	0.2	1.65	3.3
5	3	0.49	0.66	1.00
3	3	0.62	0.53	0.81

As pointed out before, the value of F_{sc} depends on the number of the connected WTGs. Considering a base value when all WTGs are in service, F_{sc} with half of the WTGs is about 75% and it is 25% when 10% of the WTGs are in service.

Figure 4-7 shows the response of the test system with SCR of 5 with half of the WTGs connected with two settings of the PI controller. The first setting is based on having all WTGs in service, and the second one is based on connecting only half of the WTGs (lower F_{sc}). It can be shown that there is no significant difference in response in the POI voltage. However, using the settings based on all WTGs would make the response a little slower since F_{sc} with half WTGs in service is lower than that calculated based on all turbines. Therefore, the K_i and K_p settings determined when all WTGs are in service can be reasonably used with 50% of WTGs. With a further lower number of connected WTGs, the settings would lead to a much faster response, and so should be revised or at least used with careful consideration.



PI control settings tuned based on having all WTGs in service



PI control settings tuned based on having half of the WTGs in service

Figure 4-7. System response with VAR control for different PI controller settings with half of the WTGs in service (static excitation, SCR=5).

4.1.4 Test Cases

Test cases with one aggregate WTG were investigated. The same capacitive load impedances applied with DFIG test cases were used here with a synchronous machine utilizing a static-type excitation system. The VAR control parameters listed in Table 4-3 were applied. The scenarios explored can be summarized as follows.

- Scenario 1: The wind farm has full power with all WTGs in service,
- Scenario 2: The wind farm has half power with all WTGs in service,
- Scenario 3: The wind farm has half power with half of the WTGs in service,
- Scenario 4: The wind farm has full power with all WTGs in service, but with different control settings. The settings determined with system SCR 20 are applied for system SCRs 5 and 3. The settings determined for system SCR 3 are applied for system SCR 20.
- Scenario 5: The wind farm has half power with all WTGs in service, but with higher initial WTG terminal voltage for system SCR 20.

4.1.5 Results Summary and Conclusions

The test cases and results are summarized in Table 4-4. The following points can be concluded:

- Scenario 1: With full power from the wind farm and all WTGs in service, a reasonable response time, of the order of a few seconds, of the POI voltage was obtained. The response with higher system SCR is slightly slower.
- Scenario 2: With half power from the wind farm and all WTGs in service, a similarly reasonable time response was also obtained with slightly longer time constant compared to scenario 1. The initial voltage of the WTG terminal voltage in this scenario is a slightly lower than that with the full power wind farm. Consequently, the operating field voltage level is lower and less voltage margin is available. This happened with system SCR 20 where the minimum field voltage limit was reached and the POI voltage response has slight overshoot. The shape or trajectory of the system response depends on the duration for which the field voltage was kept at the limit and on the time response of the excitation system itself.
- Scenario 3: With half power from the wind farm and half of the WTGs in service, a reasonable response time was obtained with system SCRs 5 and 3. With SCR 20, the POI voltage response has small overshoot and does not settle within the 20-second time window. The WTG field voltage response did not hit the limit, but was slightly slower than scenario 1 with all WTGs in service due to the slightly less than optimal tuning of the PI controller since the settings were based on the presence of all WTGs in service.
- Scenario 4: With VAR control settings for system SCR 20 applied for system SCRs 5 and 3, the value of K_i is higher than what it should be to cancel the WTG excitation time constant. The value K_i compensates for a lower value of F_{sc} . This would overcompensate the excitation system and make the VAR control faster and therefore, an oscillating response was obtained. This shows that applying the VAR control settings obtained with higher system SCR to lower system SCR could lead to underdamped or possible unstable behaviour. When the control settings for system SCR 3 were applied for system SCR 20, the K_i value is lower and the VAR control response was much slower but stable. It is clear here that there is a tradeoff between performance of the system and robust stability properties in the presence of grid impedance variations.
- Scenario 5: The same as scenario 2 with SCR 20, but with higher initial WTG voltage. The field voltage was higher and thus a larger field voltage margin was available. The field voltage minimum limit was just hit for a very short time that could still provide a smooth response and the slight overshoot observed in case 4 in scenario 2 was eliminated.

With higher system SCR, the system performance can push the field voltage towards the limit in some cases. If this happens, the system performance is highly affected by the control settings and the excitation response. Therefore, the VAR control parameters should be carefully tuned. It might be beneficial to consider if other passive elements are needed to contribute to the VAR control process, so that the WTG excitation system is not pushed to the limit with the possibility of undesired responses.

It is of importance to note that the WTG reactive power capability, with all WTGs online (156.9 MVAR), was exceeded in cases 1 and 4 as well as in case 7 with half of the WTGs (78.45 MVAR) with system SCR 20. This happened because no reactive power limits could be imposed in the VAR control loop. In order to do that, a reactive power control loop can be

implemented to be able to take care of the WTG reactive power capability as will be shown in the next section.

Table 4-4. Summary results of test cases for VAR control with static excitation of synchronous WTG implementing only voltage control

Scenario	Case	SCR	MVA base WTG1 (MW)	P WTG1 (MW)	Initial Q WTG1 (MVAR)	Initial voltage WTG1 (pu)	Load applied impedance (pu)	Q final WTG1 (MVAR)	Settling time (sec)	Notes
1	1	20	360	324	5.261	1.026	-0.5	-160.165	4	
1	2	5	360	324	5.261	1.026	-2	-40.458	3.1	
1	3	3	360	324	5.261	1.026	-3.5	-21.259	3.2	
2	4	20	360	162	-3.743	1.017	-0.5	-176.381	4.6	
2	5	5	360	162	-3.743	1.017	-2	-51.191	4.3	
2	6	3	360	162	-3.743	1.017	-3.5	-31.217	3.8	
3	7	20	180	162	8.851	1.029	-0.5	-143.652	999	
3	8	5	180	162	8.85	1.029	-2	-37.951	4.1	
3	9	3	180	162	8.851	1.029	-3.5	-18.443	3.3	
4	10	3	360	324	5.261	1.026	-3.5	-27.432	999	Settings of SCR 20 were applied to SCR 3
4	11	5	360	324	5.261	1.026	-2	-40.583	2.8	Settings of SCR 20 were applied to SCR 5
4	12	20	360	324	5.261	1.026	-0.5	-147.6373	999	Settings of SCR 3 were applied to SCR 20
5	13	20	360	162	41.945	1.043	-0.5	-140.094	5.7	Higher initial WTG terminal voltage

*Settling time of 999 sec indicates inability to recover the POI voltage to the steady state value

4.1.6 Wind Farm VAR Control with WTG Reactive Power Control Implementation

The wind farm VAR control performed in the previous subsection using the WTG voltage control does not take into account the generator reactive power capability, which could be exceeded in order to bring the voltage back to the required level after any disturbance. To overcome this limitation, a reactive power control loop with reactive power limits can be implemented using a PI controller as shown in. Figure 4-8. The excitation-generator dynamic is approximated by a first order system with a time constant T_v .

The values of the WTG reactive power limits (Q_{max}, Q_{min}) and terminal voltage limits (V_{WTG_max}, V_{WTG_min}) were assumed as in the DFIG machine. The reactive power limits are considered fixed based on a power factor of 0.9. The limits could be adapted to the machine operating point. By considering the machine power voltage (PV) curve, the reactive power capability can be extracted and compared to the reference reactive power required for VAR control (Q_{ref}). If the reference value is within the machine capability, it is used to determine the WTG reference voltage (V_{WTG_ref}). If Q_{ref} is beyond the machine capability at the operating point, Q_{ref} is limited to the machine reactive power capability.

The parameter F_n represents the portion of WTGs online. As explained with the DFIG control, this parameter adjusts the loop gain to maintain the same wind farm VAR time constant with different numbers of WTGs online.

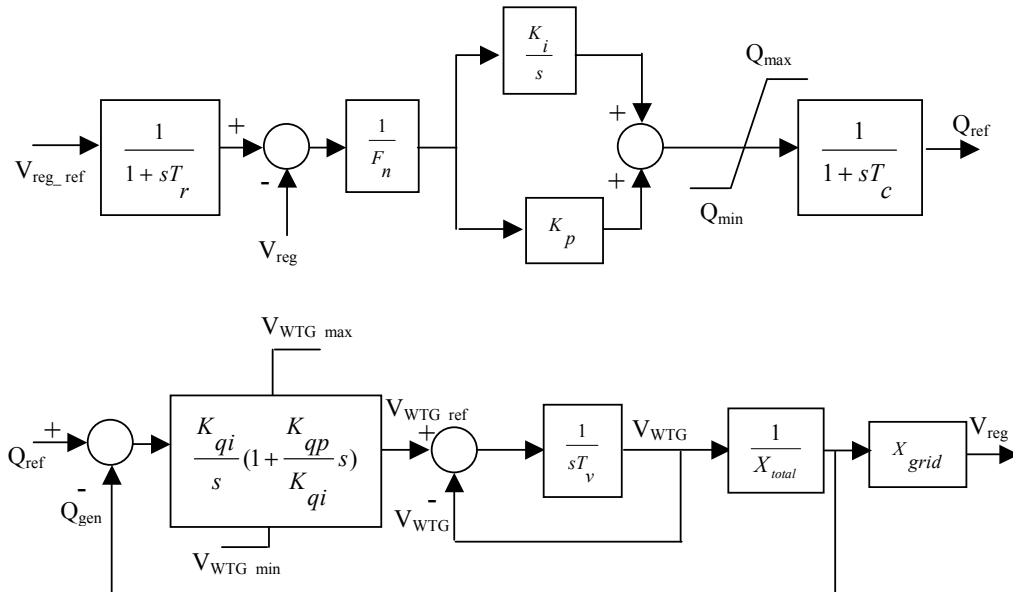


Figure 4-8. Wind farm VAR control block diagram for synchronous machine WTG.

4.1.7 Reactive Power Control Loop

The WTG voltage control loop with a synchronous machine is not as fast as that of a DFIG with power electronic grid interface. This suggests a modification to the design of the reactive power controller to be of proportional-integral (PI) type rather than of an integral type controller as that with the DFIG machine.

Given knowledge of the time constant of the WTG voltage control loop (T_v) and setting the desired time constant of the reactive power control loop (T_q), the PI controller parameters can be determined such that K_{qp}/K_{qi} cancels T_v , and K_{qi} can be set based on T_q as follows:

$$\frac{K_{qp}}{K_{qi}} = T_v \quad (5.2)$$

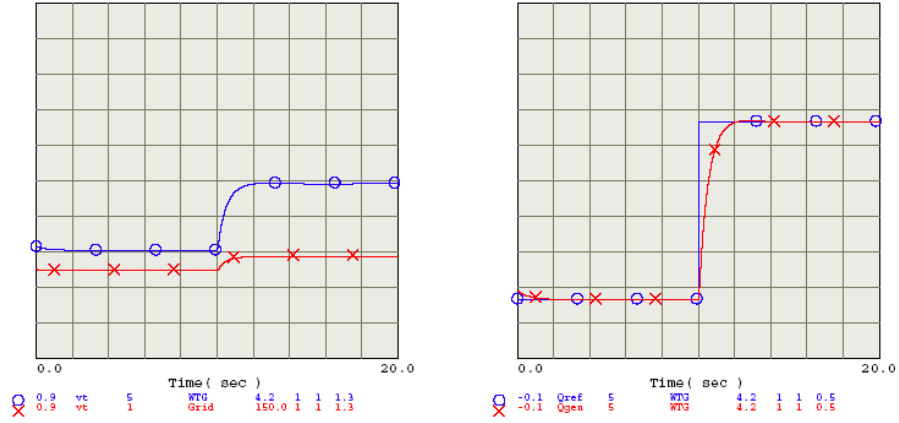
$$K_{qi} = \frac{X_{total}}{T_q} \quad (5.3)$$

It is clear that the system SCR has an impact on the controller since it affects the total system reactance as observed from the equivalent WTG terminal (X_{total}). Table 4-5 lists the WTG reactive power controller parameters. X_{total} was calculated with all WTGs online. The range of variation of X_{total} depends on the percentage of WTGs online.

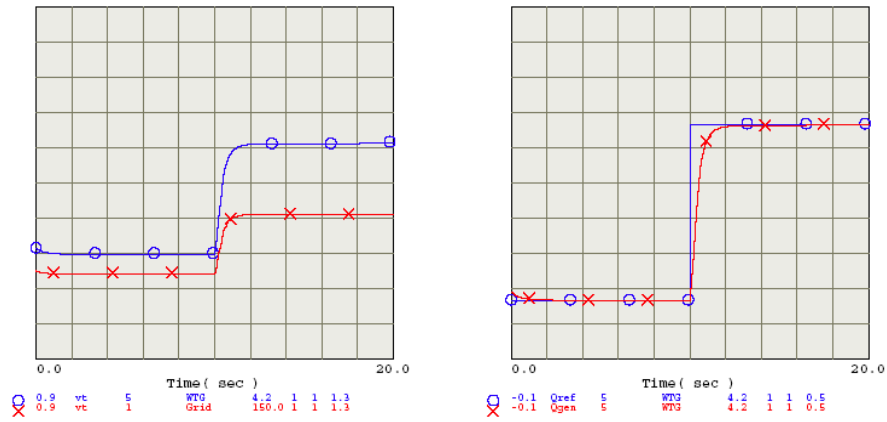
From the previous investigation of the static excitation performance, the WTG voltage control time constant was set to 1 second. The reactive power control loop time constant was set to 0.5 seconds. The response of the test system to a step change of 0.3 pu of the aggregate WTG reference reactive power (Q_{ref}) for different system SCRs is depicted in Figure 4-9. The full power wind farm was considered with all WTGs online (324 MW). The figure shows the voltage of the WTG (o marks) and the POI voltage (x marks). The WTG voltage limits were not applied to investigate the response of the reactive power control, which was acceptable according to the desired time constant.

Table 4-5 WTG reactive power control loop parameters with static excitation system

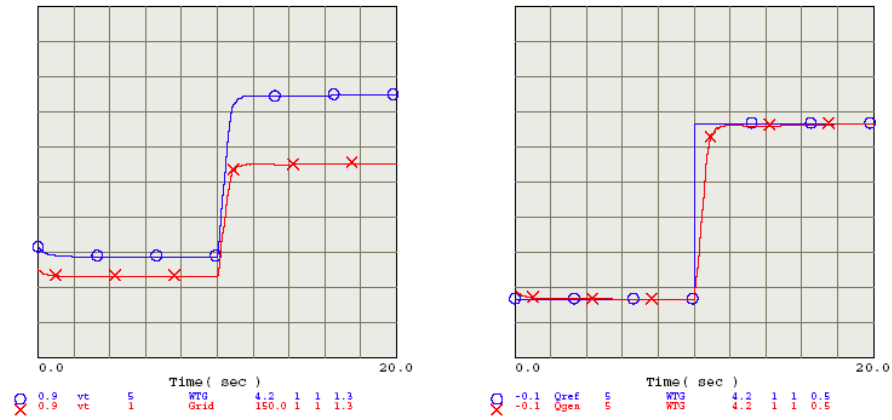
SCR	T_q (sec)	K_{qi}	K_{qp}
20	0.5	0.5	0.5
5	0.5	0.82	0.82
3	0.5	1.08	1.08



SCR:20



SCR:5



SCR:3

Figure 4-9. System response with static excitation of synchronous WTG to a 0.3 pu step change of the reference WTG reactive power (324 MW, all WTGs in service).

4.1.8 Wind Farm VAR Control Loop

The wind farm control loop involves the WTG voltage and reactive power control loops. The wind VAR controller is a PI controller that regulates the voltage at the POI. The controller parameters can be determined following the same guidelines as for the DFIG. The value of K_i is set according to the desired time constant of the wind farm VAR control (T_{var}) and the grid

reactance (X_{grid}). The ratio K_p/K_i is chosen to cancel the reactive power control loop time constant T_q . This can be interpreted as follows:

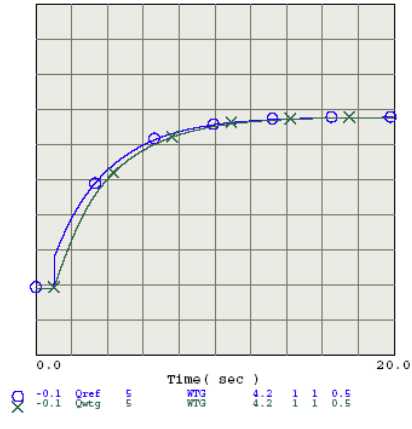
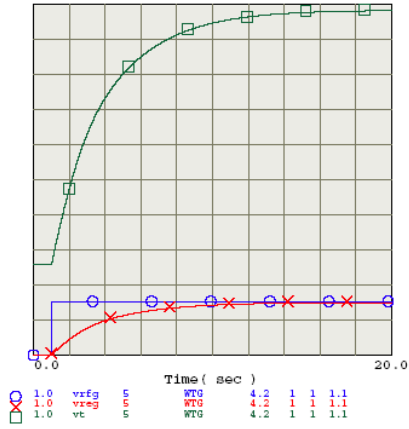
$$\frac{K_p}{K_i} = T_q \quad (5.4)$$

$$K_i = \frac{1}{T_{var} \cdot X_{grid}} \quad (5.5)$$

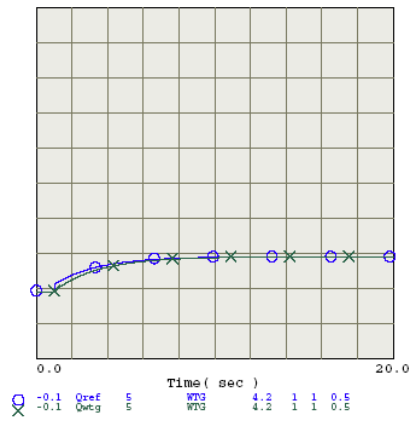
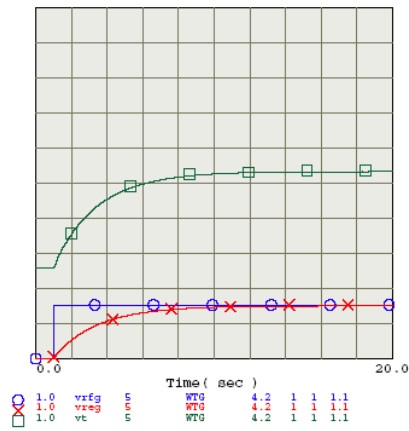
The wind farm VAR controller parameters are shown in Table 4-6. The system response to a step change of the reference voltage at the POI (V_{ref}) is shown in Figure 4-10 with all WTGs in service and in Figure 4-11 with half of the WTGs in service. V_{reg} is the regulated voltage at the POI and V_t is the WTG terminal voltage. With all WTGs connected, the step voltage magnitude was 0.015 pu where it was 0.01 pu with half of the WTGs in service so that the WTG reactive power does not exceed the machine maximum limit. A reasonable time response (settling time of the order of a few seconds) of the POI voltage with the desired time constant was obtained.

Table 4-6 Wind VAR control loop parameters with static excitation system

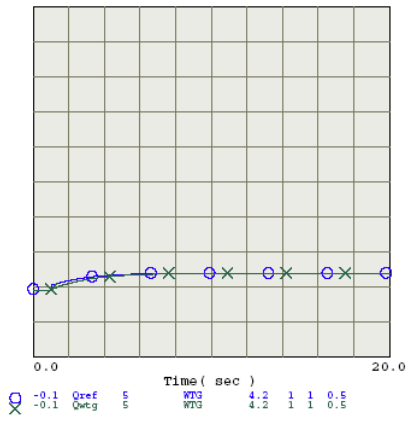
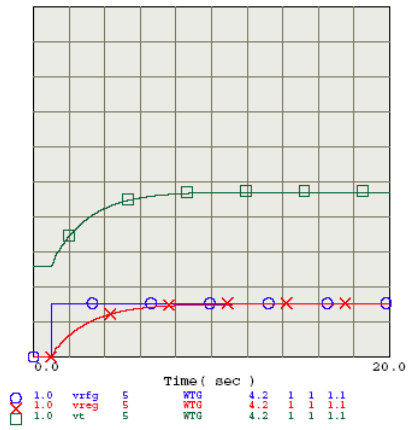
SCR	T_{var} (sec)	K_i	K_p
20	3	6.66	3.33
5	3	1.66	0.833
3	3	1.0	0.5



SCR:20

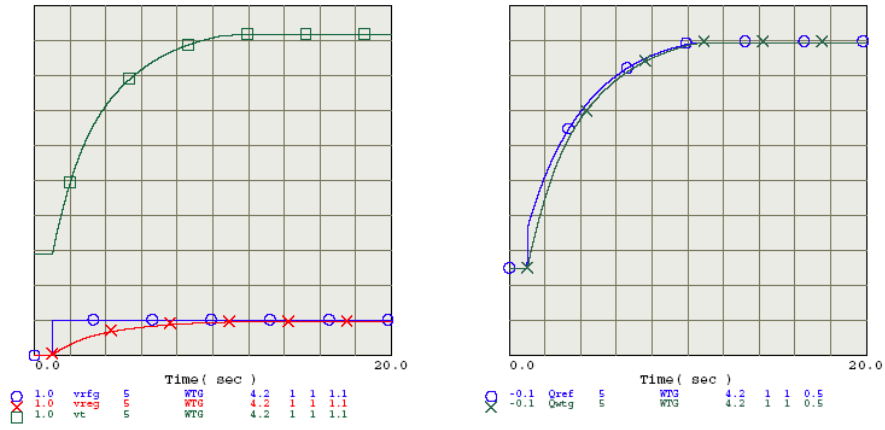


SCR:5

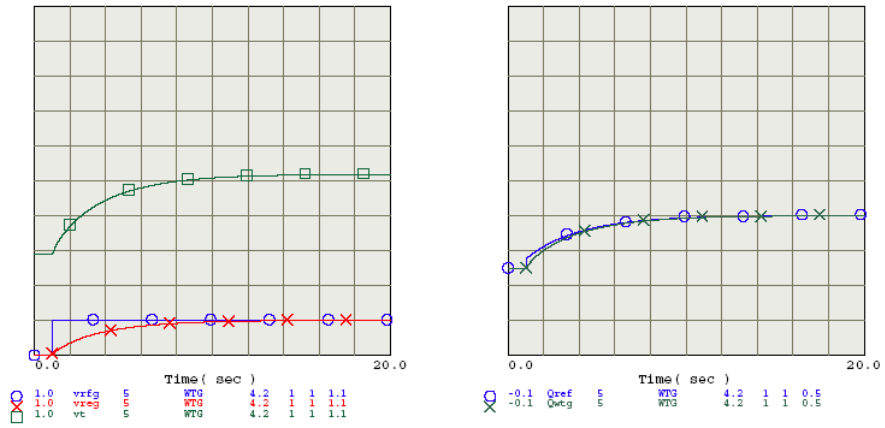


SCR:3

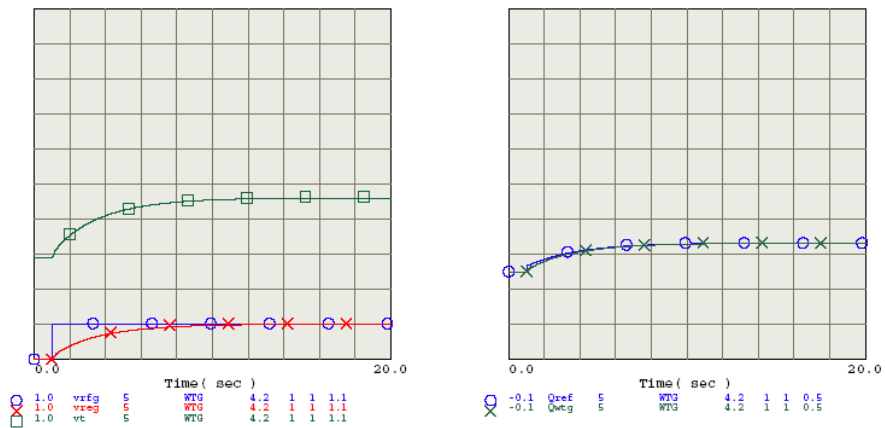
Figure 4-10. System response with static excitation of synchronous WTG to a regulated voltage step change (v_{rfg}) for different SCRs (all WTGs in service with $F_n=1$).



SCR:20



SCR:5



SCR:3

Figure 4-11. System response with static excitation of synchronous WTG to a regulated voltage step change (v_{rfq}) for different SCRs (half of WTGs in service with $F_n=0.5$).

4.1.9 Test Cases and Results

The same test cases performed for the synchronous machine with WTG voltage control strategy were explored with the implementation of the WTG reactive power control. The test cases and results are summarized in Table 4-7.

With the reactive power control loop, the same general conclusions as before can be drawn as for only the voltage control loop:

- The POI voltage response with the reactive power control implementation is slightly slower than that obtained with only the voltage control loop.
- The WTG reactive power limits were explicitly incorporated into the control to ensure that the reactive power lies within the generator capability. However, this prevented the POI voltage in some case, with system SCR 20, from recovering back to the desired steady state value as occurred in cases 4 and 7. In both cases, there was a requirement that the WTG absorbs more reactive power.
- As observed before, applying the control settings of higher system SCR to a lower one would result in a faster response (cases 10 and 11) and vice versa (case 12).
- With higher initial WTG voltage (case 13), more reactive power capability was available to regulate the POI voltage to the reference value.

Table 4-7. Summary results of test cases for VAR control with static excitation of synchronous WTG implementing reactive power control

Scenario	Case	SCR	MVA base WTG1 (MW)	P WTG1 (MW)	Initial Q WTG1 (MVAR)	Initial voltage WTG1 (pu)	Load applied impedance (pu)	Q final WTG1 (MVAR)	Settling time (sec)	Notes
1	1	20	360	324	5.261	1.026	-0.5	-156.808	5.9	
1	2	5	360	324	5.261	1.026	-2	-40.653	6	
1	3	3	360	324	5.261	1.026	-3.5	-21.323	5.4	
2	4	20	360	162	-3.743	1.017	-0.5	-156.684	999	
2	5	5	360	162	-3.743	1.017	-2	-51.351	3.6	
2	6	3	360	162	-3.743	1.017	-3.5	-31.29	3.7	
3	7	20	180	162	8.851	1.029	-0.5	-78.456	999	
3	8	5	180	162	8.85	1.029	-2	-38.313	6.6	
3	9	3	180	162	8.851	1.029	-3.5	-18.586	6.4	
4	10	3	360	324	5.261	1.026	-3.5	-21.321	1.2	Settings of SCR 20 were applied to SCR 3
4	11	5	360	324	5.261	1.026	-2	-40.638	1.6	Settings of SCR 20 were applied to SCR 5
4	12	20	360	324	5.261	1.026	-0.5	-116.441	999	Settings of SCR 3 were applied to SCR 20
5	13	20	360	162	41.945	1.043	-0.5	-142.062	5.6	Higher initial WTG terminal voltage

*Settling time of 999 sec indicates inability to recover the POI voltage to the steady state value

4.2 Brushless-Type Excitation System

A brushless-type excitation system has a rotating diode bridge rectifier on the same shaft with the exciter armature and the main generator field. Therefore, the need for slip ring and brushes is eliminated. The DC output from the rotating rectifier is directly fed to the main generator field. The stationary field voltage of the exciter is controlled and consequently the AC exciter voltage is regulated, which in turn controls the DC field of the main generator through the diode bridge rectifier. The excitation system time response has an impact on the system response and the design of the VAR control. It is supplied from the main generator voltage and, therefore, is affected by grid disturbance events.

4.2.1 Performance of Brushless-Type Excitation System

The block diagram of the brushless-type excitation system is shown in Figure 4-12. The control is performed using a PID controller. The parameters of the excitation system are listed in Table 4-8 [6].

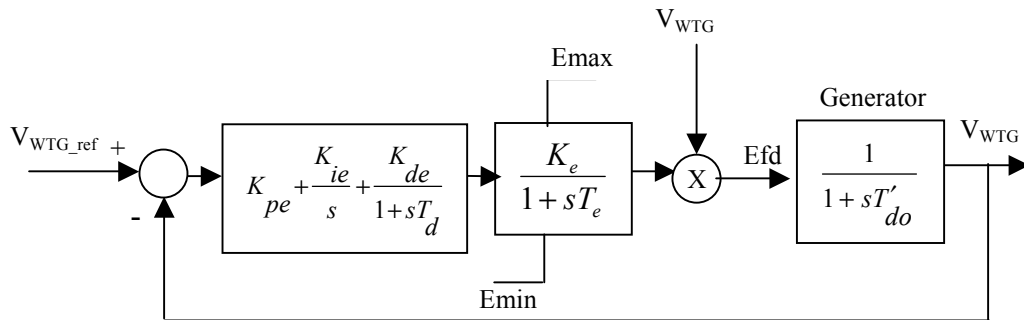


Figure 4-12. Brushless excitation control block diagram.

Table 4-8. Parameters of control block diagram of brushless excitation system.

Parameter	Description	Value
T_d	Voltage regulator derivative time constant (sec)	0.1
T_b	Denominator time constant of lead-lag block (sec)	30
K_{pe}	Voltage regulator proportional gain	40
K_{ie}	Voltage regulator integral gain	7
K_{de}	Voltage regulator derivative gain	20
K_e	Exciter field proportional constant	1
T_e	Exciter field time constant (sec)	1.2
T'_{do}	Direct axis transient generator time constant (sec)	6.5

The open loop frequency response characteristic of the brushless excitation system is shown in Figure 4-13. The response has an infinite gain margin, and a phase margin of 61° at the 0dB cross over frequency of 3.15 rad/sec. The closed loop system is stable with fast time response achieved through the tuning of the excitation system control parameters.

The closed loop Bode plot is shown in Figure 4-14. The 3dB bandwidth is 4.82 rad/. The peak value of the gain is about 0.97 dB at 1.83 rad/sec. The absence of a dominant resonant peak confirms the damped nature of the voltage response with very little voltage overshoot. This satisfies the recommended value in the IEEE Std. 421.2-1990 for guidance towards the evaluation of dynamic response of excitation control systems [7].

The response to a step capacitive load impedance, with values similar to those applied to investigate the performance of static-type excitation system, is shown in Figure 4-15 with all WTGs in service and in Figure 4-16 with half of the WTGs. The response of the WTG terminal voltage is relatively damped for both cases and is slightly faster with all WTGs connected but the difference is not significant.

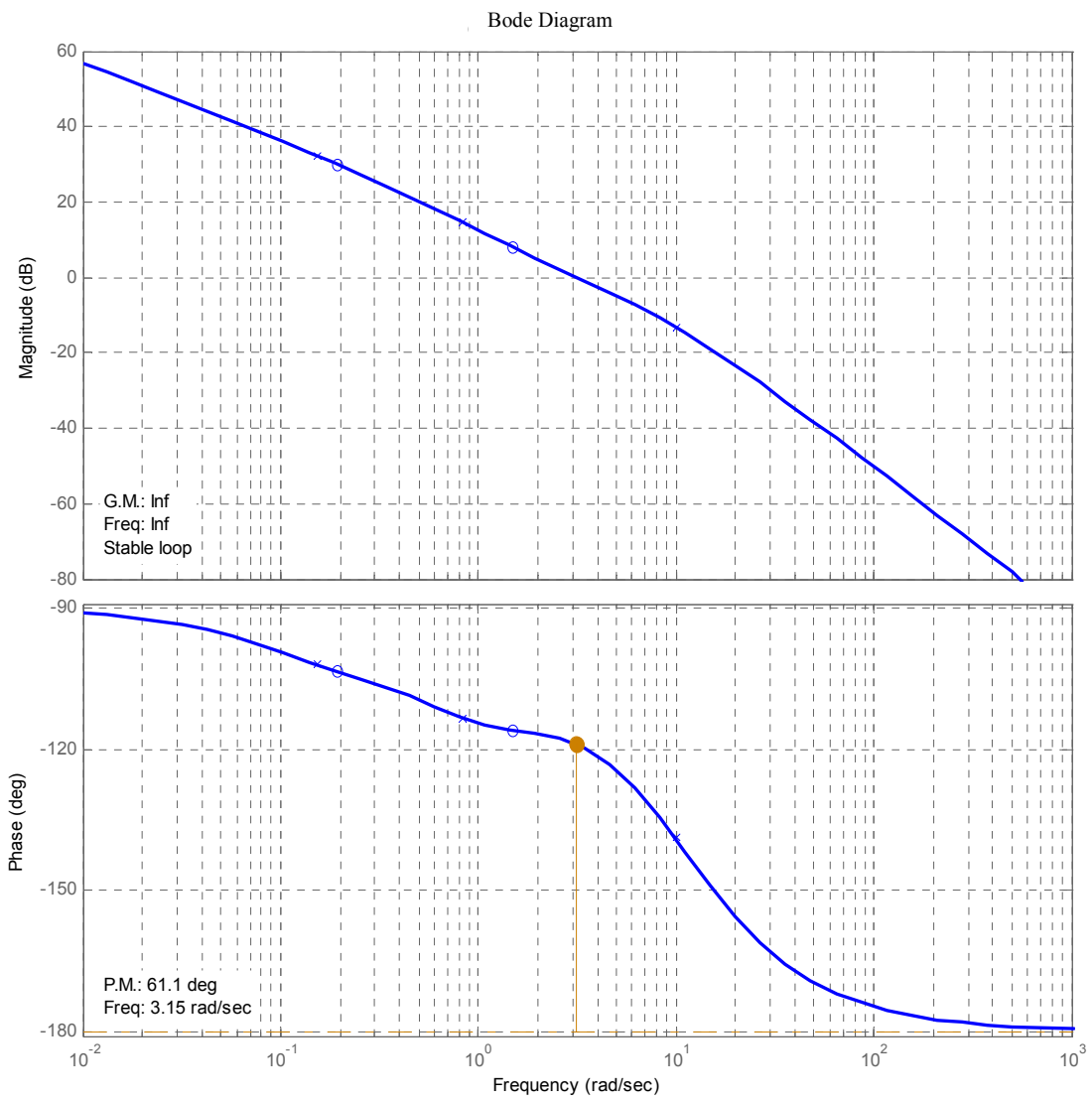


Figure 4-13. Open loop Bode diagram of the brushless excitation system.

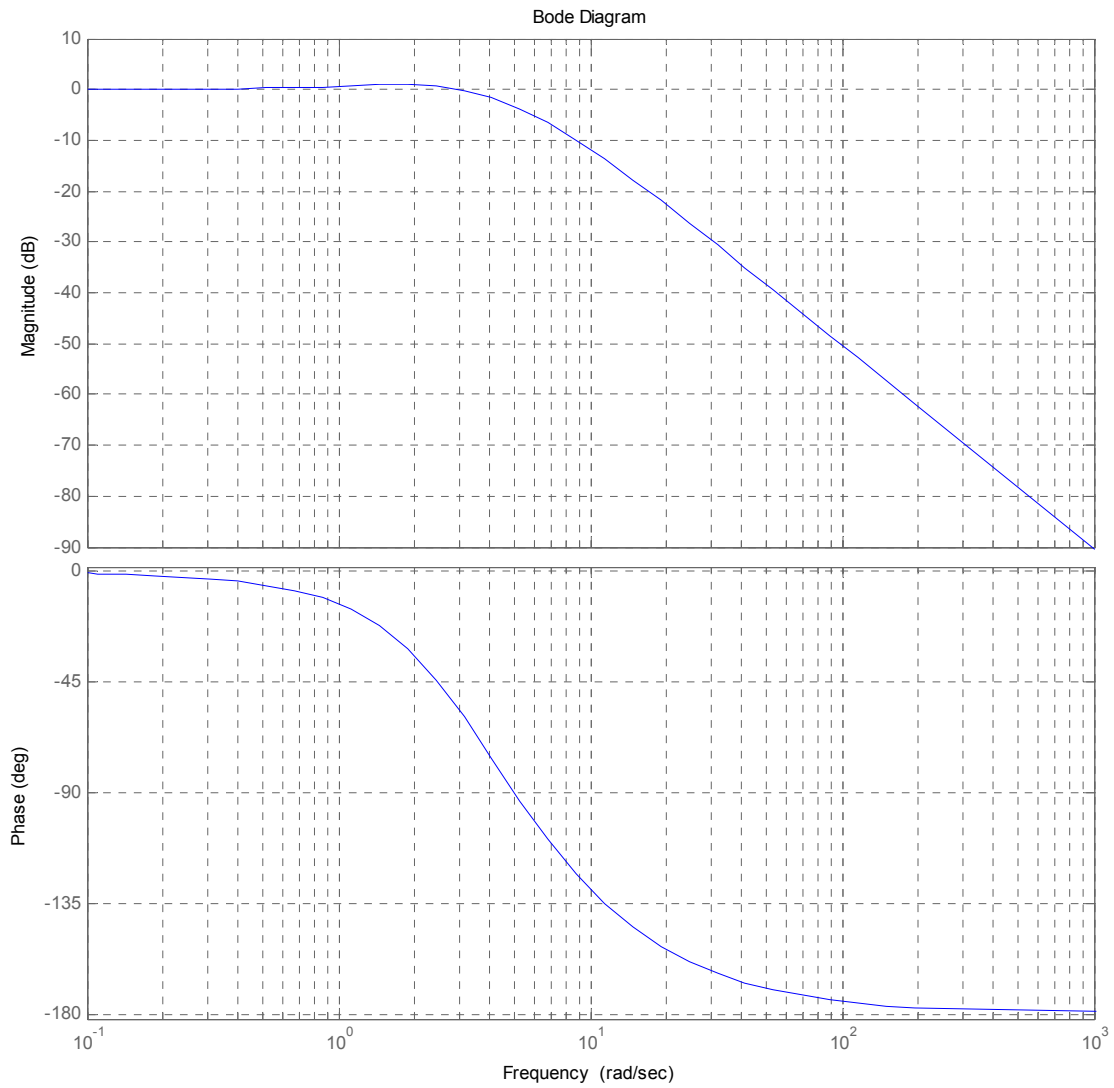
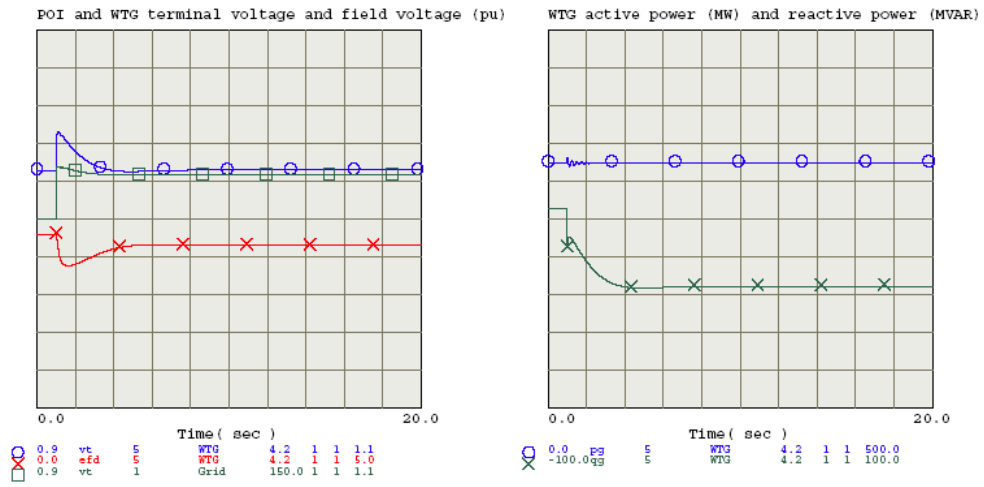
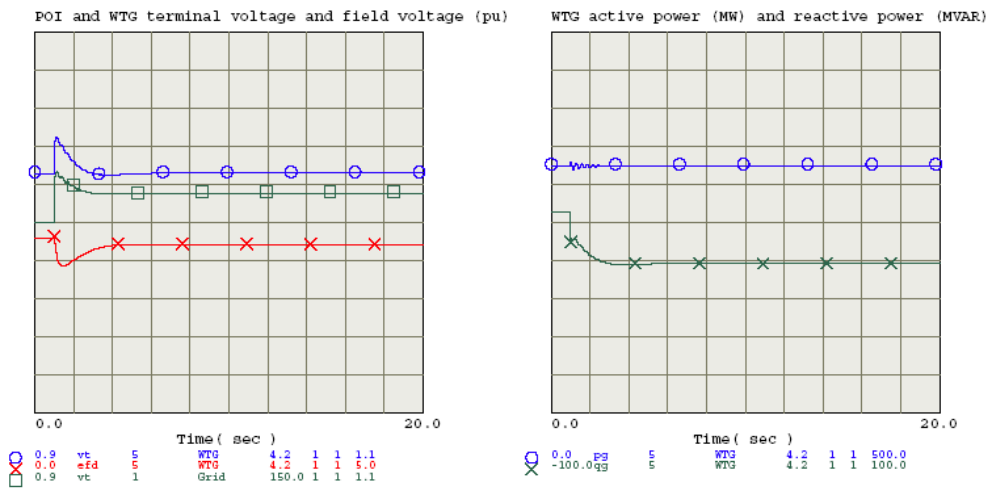


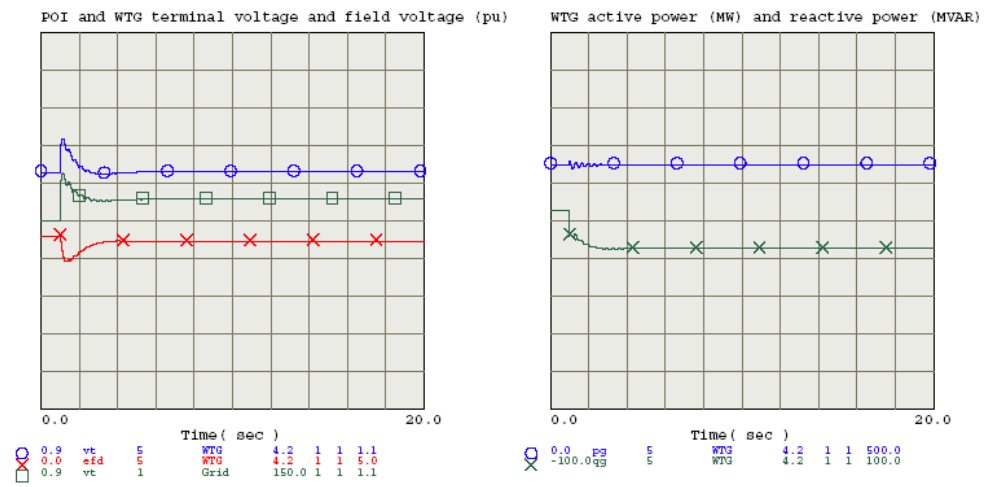
Figure 4-14. Closed loop Bode diagram of the brushless excitation system.



SCR:20

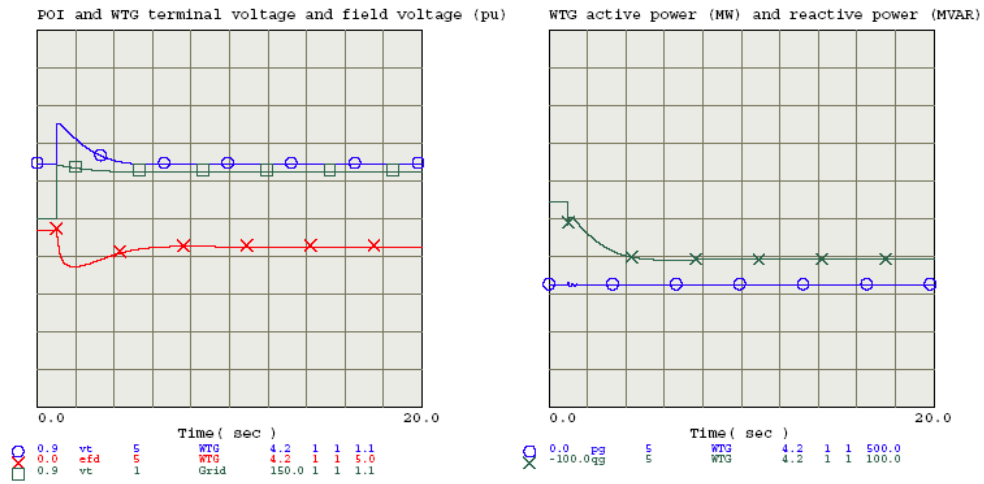


SCR:5

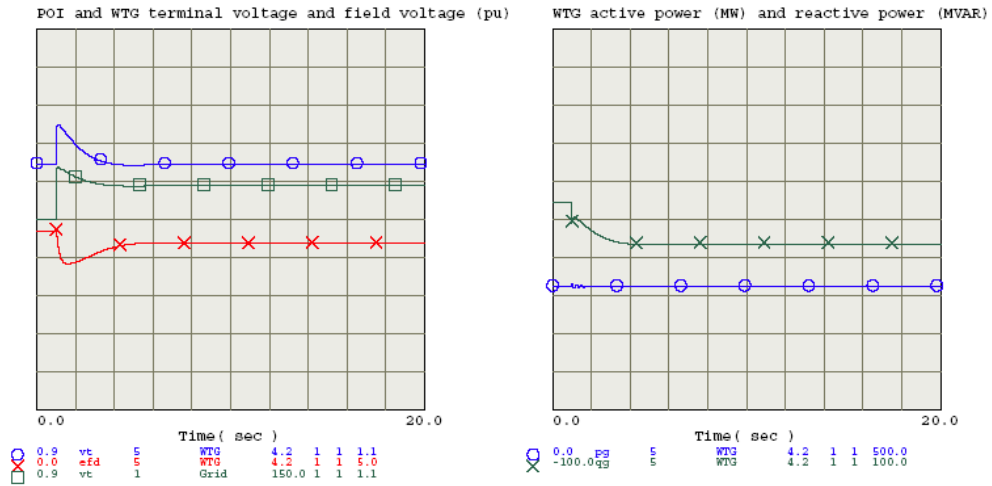


SCR:3

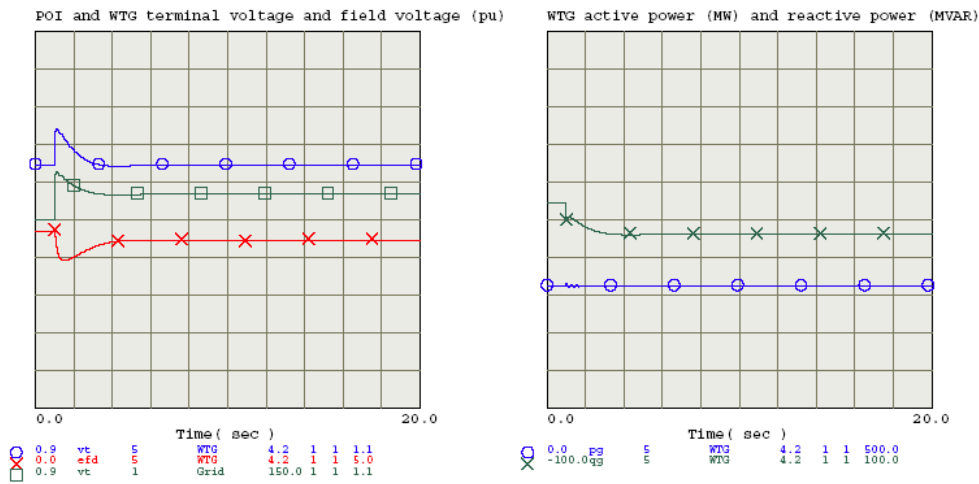
Figure 4-15. Brushless excitation system response with all WTGs in service (324 MW).



SCR:20



SCR:5



SCR:3

Figure 4-16. Brushless excitation system response with half of the WTGs in service (162 MW).

4.2.2 Wind Farm VAR Control using WTG Voltage Control

The VAR control implementation is performed as before with the static excitation system through a PI controller to regulate the voltage at the POI bus. The control block diagram is illustrated in Figure 4-17. With the PID controller of the excitation system, the reference of the WTG terminal voltage is equal to the WTG voltage in the steady-state condition.

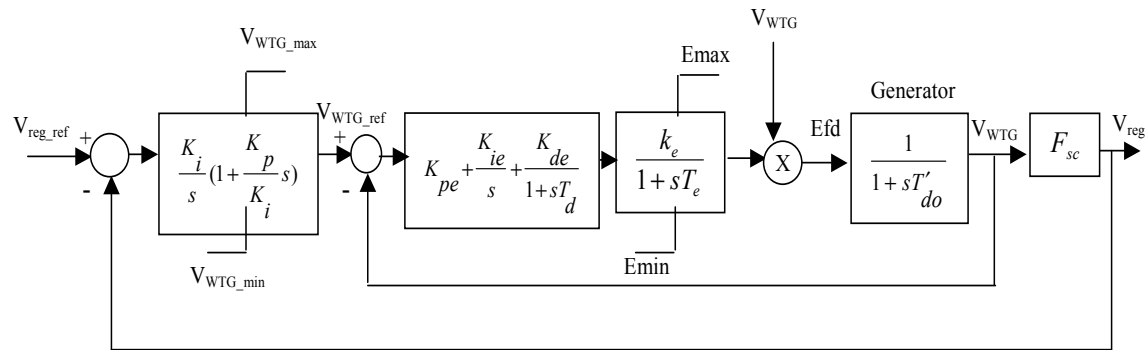


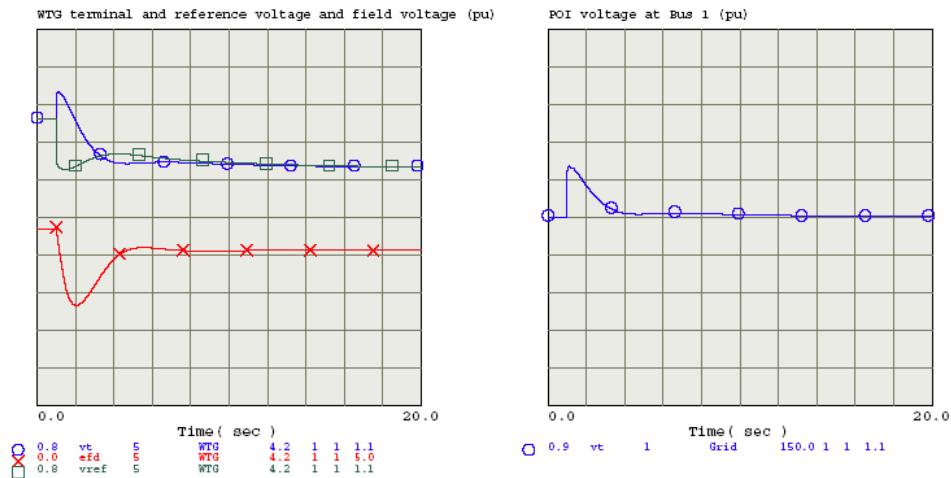
Figure 4-17. Wind farm VAR control block diagram with brushless excitation system.

The selected PI control parameters are listed in Table 4-9. T_{var} was set to 3 seconds with system SCRs 3 and 5. It was set to 5 seconds with SCR 20 to avoid voltage collapse associated with the slower response of the excitation system when half of the WTGs are online. The value of K_p/K_i was set to 2 for all cases, which is the estimated time constant of the excitation system without the VAR control implementation.

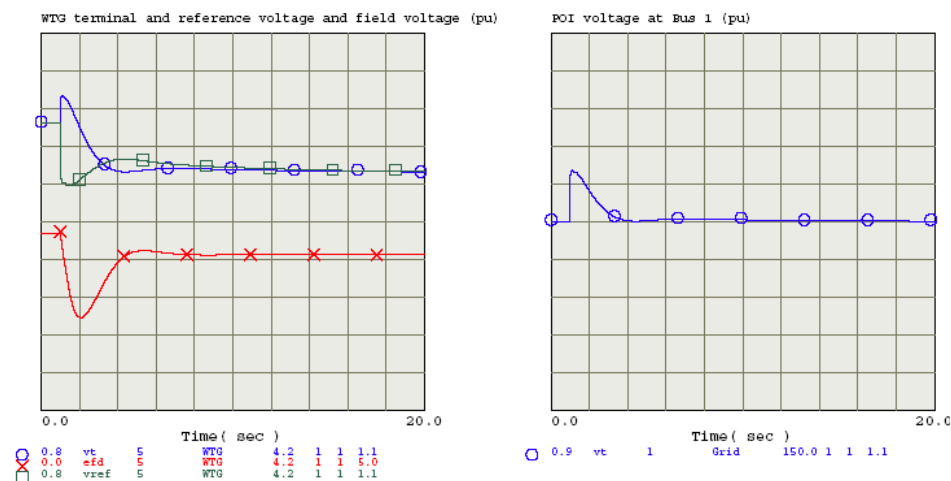
Table 4-9. VAR control parameters with brushless excitation system

SCR	T_{var} (sec)	F_{sc}	K_i	K_p
20	5	0.2	1	2
5	3	0.49	0.67	1.35
3	3	0.62	0.53	1.07

As noted previously, adjusting F_{sc} with the variation of the number of connected WTGs till 50% would not have a significant impact due to the small variation of the F_{sc} value for the same system SCR. Figure 4-18 shows the system response with SCR of 5 with half of the WTGs in service with and without adjusting F_{sc} . The figure confirms the previous assumptions where there is no noticeable response difference. Therefore, the control settings listed in Table 4-9, which are determined with all WTGs in service, can be used as the default settings. However, with further lower portion of connected WTGs, the settings should be adjusted.



PI control settings tuned based on having all WTGs in service



PI control settings tuned based on having half of the WTGs in service

Figure 4-18. System response with VAR control for different PI controller settings with half of the WTGs in service (brushless excitation, SCR=5).

4.2.3 Test Cases and Conclusions

The same test cases conducted with the static excitation system were investigated with the brushless-type. The results are summarized in Table 4-10.

Generally, when the control parameters are within the excitation system field voltage capability and the WTG voltage limits, the desired response can be obtained. But with higher system SCR, the minimum limit of the WTG voltage or the limit of the field voltage can be reached. This can happen with lower WTG initial voltage which implies lower margin to the minimum field voltage limit.

The following conclusions can be drawn:

- Scenario 1: With full power wind farm and all WTGs in service, a reasonable response time (a few seconds) for the POI voltage was obtained for system SCRs 5 and 3. The settling time was long for SCR 20. This was mainly due to the intentionally larger time response of the VAR control to prevent voltage collapse for scenario 3.
- Scenario 2: With half power wind farm and all WTGs in service, a reasonable response was also obtained for system SCRs 5 and 3. The settling time was longer for SCR 20.

- Scenario 3: With half power wind farm and half of WTGs in service, a reasonable response was obtained with system SCRs 5 and 3. With system SCR 20, a voltage collapse occurred when K_i was determined using a 3 seconds VAR control time constant. This is shown in Figure 4-19. The WTG terminal voltage reacts on a fast time scale the excitation system reacts relatively slowly, and so could not regulate the WTG voltage to a stable condition. In this case, the VAR control time response was slowed down where the VAR control time constant was increased and set to 5 seconds. This is achieved by having a lower value of the integral gain K_i of the PI controller while maintaining the value of K_p/K_i to cancel out the excitation system time constant. However in steady state, the POI voltage could not settle to the desired value because the WTG terminal voltage limit was reached. In order to obtain the required performance with the wind VAR control, within the excitation system capability with high SCR, coordination could be made with other passive elements.
- Scenario 4: With VAR control settings for system SCR 20 applied for system SCRs of 5 and 3, the VAR control response is faster and has a slight overshoot because the control settings were based on higher K_i making the POI voltage settle more quickly. When the control settings for system SCR 3 were applied for system SCR 20, the VAR control was slower due to the lower K_i value determined with SCR 3. The POI voltage does not settle within the 20-second window.
- Scenario 5: With higher WTG initial voltage with system SCR 20 in scenario 2, the WTG voltage has more margin before reaching voltage limits. The WTG voltage minimum limit was not reached and the settling time was slightly less than that in case 4 with lower overshoot.

The implementation of only WTG voltage control did not consider the WTG reactive power capability. This limitation is relevant in cases 4 and 7 where the final WTG reactive power exceeded the unit minimum limit. The test cases confirmed the sensitivity of the system response with higher system SCR. The brushless excitation system response might impose constraints on the VAR control. Coordination with passive elements can provide for more margin to the WTG voltage limits.

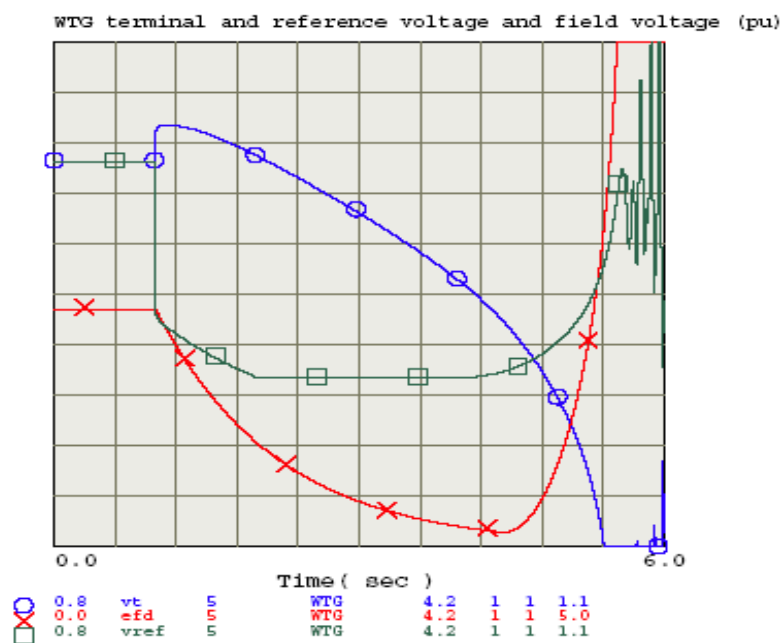


Figure 4-19. A voltage collapse case with half of WTGs for system SCR 20.

Table 4-10. Summary results of test cases for VAR control with brushless excitation of synchronous WTG implementing only voltage control

Scenario	Case	SCR	MVAbase WTG1 (MW)	P WTG1 (MW)	Initial Q WTG1 (MVAR)	Initial voltage WTG1 (pu)	Load applied impedance (pu)	Q final WTG1 (MVAR)	Settling time (sec)	Notes
1	1	20	360	324	5.261	1.026	-0.5	-157.06	11.1	
1	2	5	360	324	5.261	1.026	-2	-40.39	1.9	
1	3	3	360	324	5.261	1.026	-3.5	-21.236	1.5	
2	4	20	360	162	-3.743	1.017	-0.5	-171.338	9.6	
2	5	5	360	162	-3.743	1.017	-2	-51.097	2.5	
2	6	3	360	162	-3.743	1.017	-3.5	-31.213	2.2	
3	7A	20	180	162	8.851	1.029	-0.5			Voltage collapse occurred with $T_{var}=3$ seconds
3	7	20	180	162	8.851	1.029	-0.5	-136.072	999	
3	8	5	180	162	8.85	1.029	-2	-37.865	2.7	
3	9	3	180	162	8.851	1.029	-3.5	-18.416	2.1	
4	10	3	360	324	5.261	1.026	-3.5	-21.282	2.4	Settings of SCR 20 were applied to SCR 3
4	11	5	360	324	5.261	1.026	-2	-40.526	2.8	Settings of SCR 20 were applied to SCR 5
4	12	20	360	324	5.261	1.026	-0.5	-147.066	999	Settings of SCR 3 were applied to SCR 20
5	13	20	360	162	41.945	1.043	-0.5	-138.522	9.1	Higher initial WTG terminal voltage

*Settling time of 999 sec indicates inability to recover the POI voltage to the steady state value

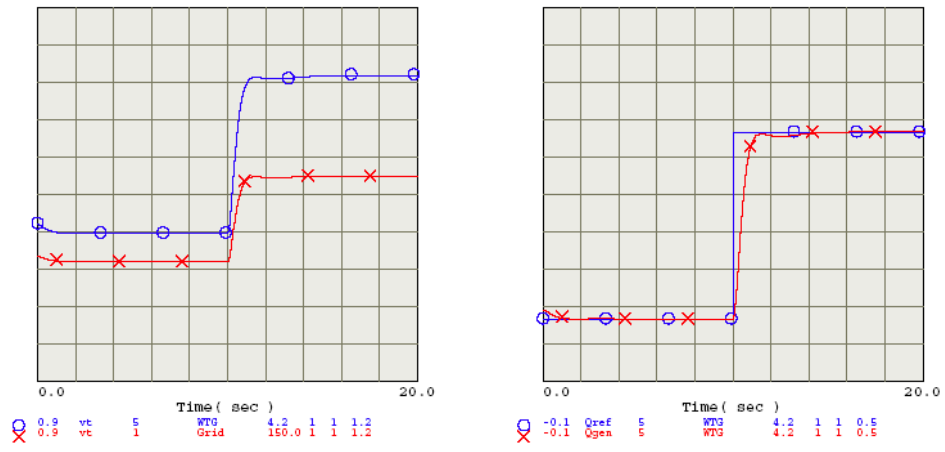
4.2.4 Wind Farm VAR Control with WTG Reactive Power Control Implementation

The same block diagram used with static-type excitation for VAR control implementing the WTG reactive power control was simulated with the brushless-type. The WTG reactive control loop considers the reactive power capability of the WTG in terms of the reactive power limits. The controller parameters were determined following the same guidelines. The values of T_q and T_{var} were set to 0.5 and 3 seconds respectively. The only difference is the time constant of each excitation type, which affects the estimation of the reactive power PI controller parameters listed in Table 4-11 considering all WTGs online. The values of K_{qi} and K_{qp} were tuned to have a reasonable response in terms of the settling time (of the order of a few seconds) to a step change of 0.3 pu of the aggregate WTG reference reactive power (Q_{ref}) as shown in Figure 4-20. The WTG voltage limits were not applied to test the reactive power loop response.

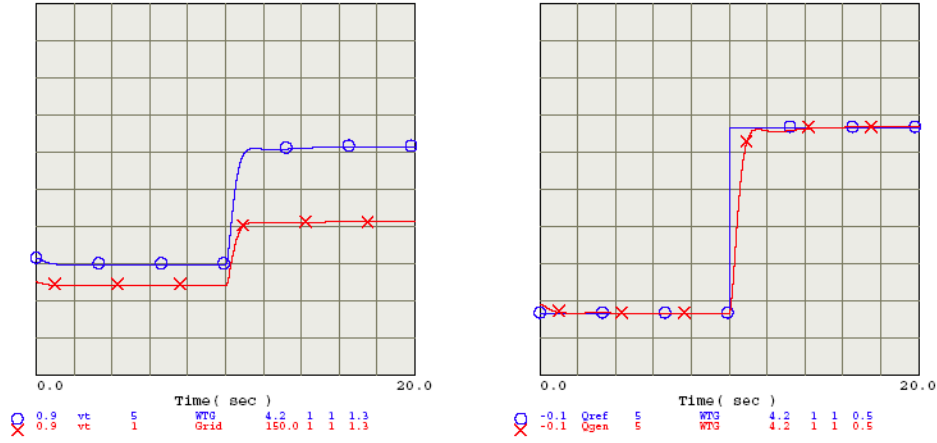
Table 4-11. Wind farm VAR control parameters with reactive power control implementation with brushless excitation system

SCR	T_q (sec)	T_{var} (sec)	K_{qi}	K_{qp}	K_i	K_p
20	0.5	3	0.5	0.45	6.66	3.33
5	0.5	3	0.82	0.5	1.66	0.833
3	0.5	3	1.08	0.45	1.0	0.5

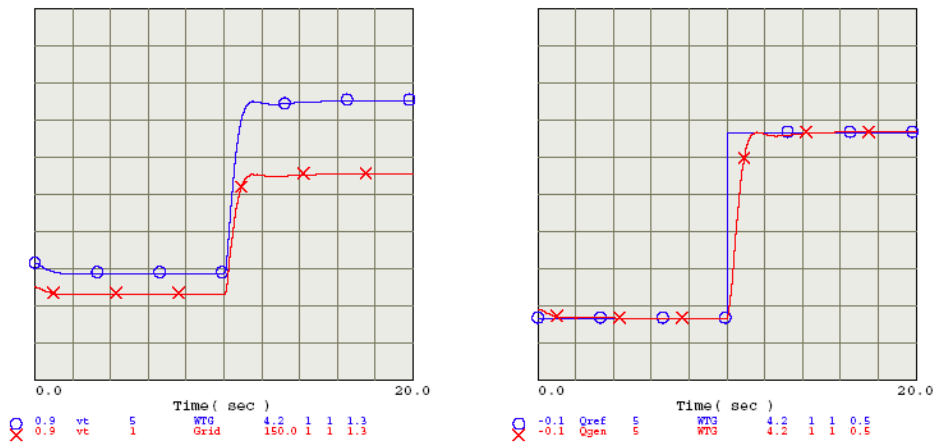
The response to the same step change of the POI voltage applied with the static-type excitation was tested for the brushless-type. A reasonable time response was obtained as shown in Figure 4-21 with all WTGs in service and in Figure 4-22 with half of the WTGs in service.



SCR:20

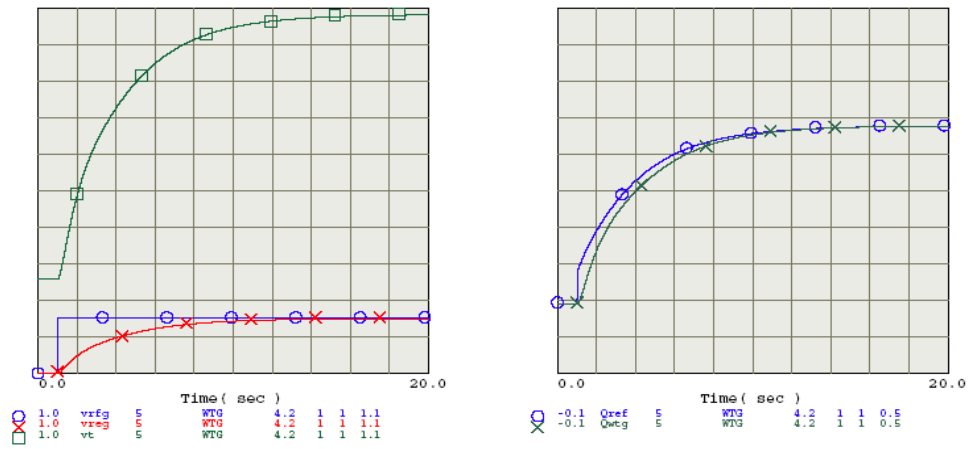


SCR:5

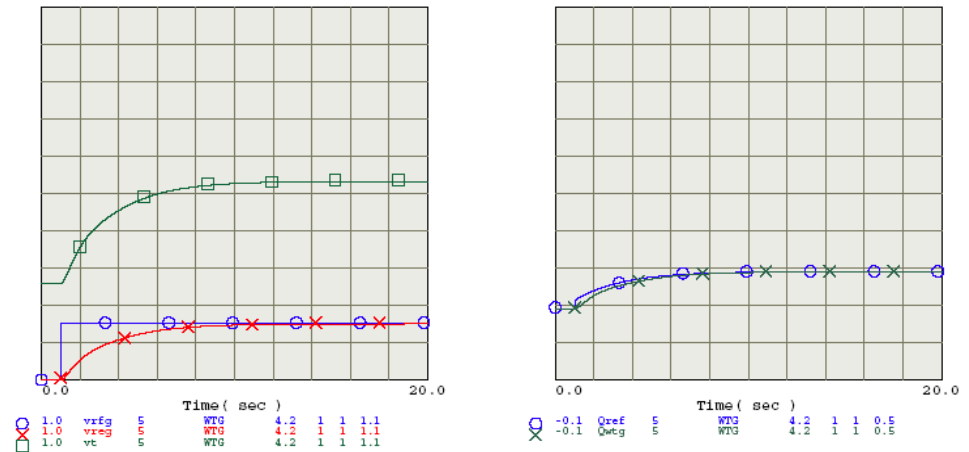


SCR:3

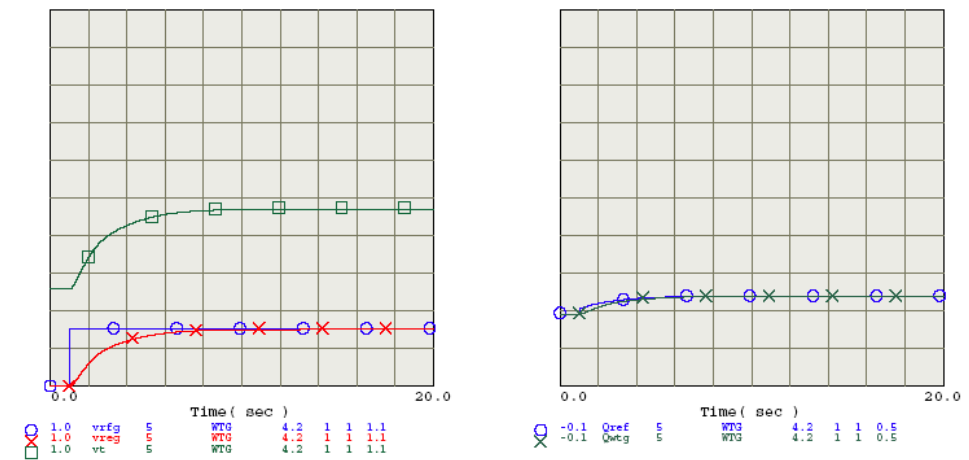
Figure 4-20. System response with brushless excitation of synchronous WTG to a 0.3 pu step change of the reference WTG reactive power (324 MW, all WTGs are in service).



SCR:20

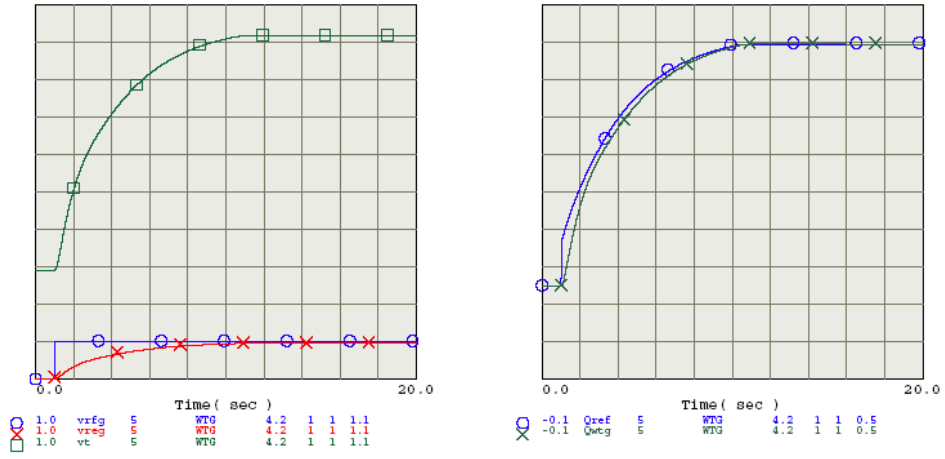


SCR:5

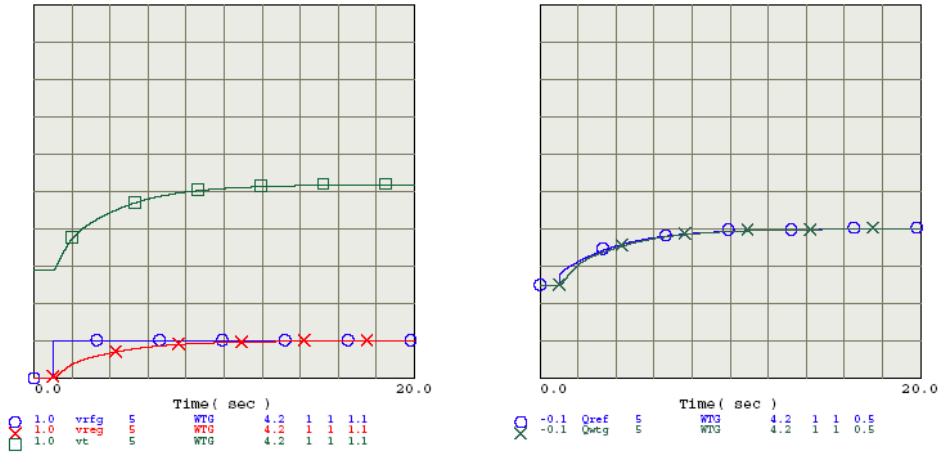


SCR:3

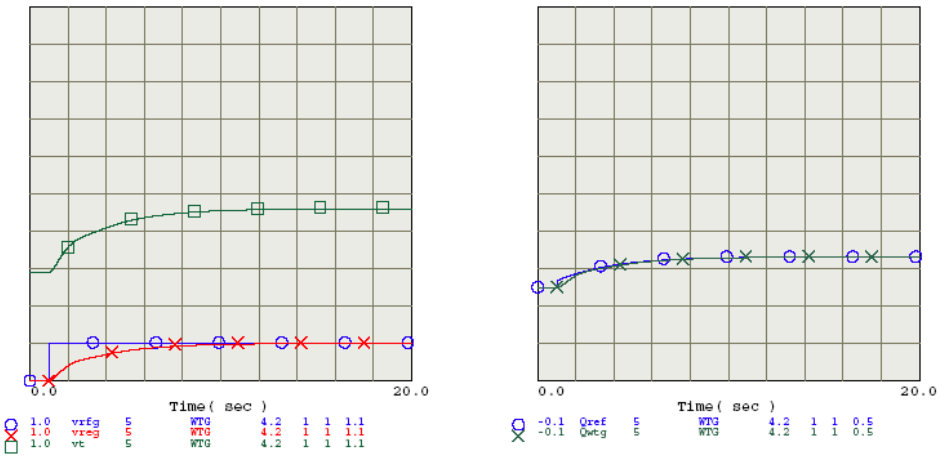
Figure 4-21. System response with brushless excitation of synchronous WTG to a regulated voltage step change (v_{rfg}) for different SCRs (all WTGs in service with $F_n=1$).



SCR:20



SCR:5



SCR:3

Figure 4-22. System response with brushless excitation of synchronous WTG to a regulated voltage step change (v_{rfg}) for different SCRs (half of WTGs in service with $F_n=0.5$).

4.2.5 Test Cases and Results

The same test cases performed with the static-type excitation were investigated with the brushless-type exciter. The results are summarized in Table 4-12.

The same general conclusions drawn before with only voltage control can be applied with the reactive power control implementation where:

- The POI voltage response with the reactive power control implementation is slightly slower than that obtained with only the voltage control.
- The WTG reactive power limits were defined by the generator capability. However this prevented the POI voltage in some cases, with system SCR 20, from achieving the desired steady state value. This happened in cases 4 and 7 due to reaching the minimum WTG reactive power limit.
- As observed before, applying the control settings of higher system SCR to a lower one would result in a faster response (cases 10 and 11) and vice versa (case 12).
- With higher initial WTG voltage (case 13), more reactive power margin was required to regulate the POI voltage.

Table 4-12. Summary results of test cases for VAR control with brushless excitation of synchronous WTG implementing reactive power control

Scenario	Case	SCR	MVA base WTG1 (MW)	P WTG1 (MW)	Initial Q WTG1 (MVAR)	Initial voltage WTG1 (pu)	Load applied impedance (pu)	Q final WTG1 (MVAR)	Settling time (sec)	Notes
1	1	20	360	324	5.261	1.026	-0.5	-156.693	6	
1	2	5	360	324	5.261	1.026	-2	-40.637	5.9	
1	3	3	360	324	5.261	1.026	-3.5	-21.323	5.3	
2	4	20	360	162	-3.743	1.017	-0.5	-155.807	999	
2	5	5	360	162	-3.743	1.017	-2	-51.356	3.8	
2	6	3	360	162	-3.743	1.017	-3.5	-31.284	3.7	
3	7	20	180	162	8.851	1.029	-0.5	-78.288	999	
3	8	5	180	162	8.85	1.029	-2	-38.3	6.5	
3	9	3	180	162	8.851	1.029	-3.5	-18.576	6.3	
4	10	3	360	324	5.261	1.026	-3.5	-21.33	1.8	Settings of SCR 20 were applied to SCR 3
4	11	5	360	324	5.261	1.026	-2	-40.639	2	Settings of SCR 20 were applied to SCR 5
4	12	20	360	324	5.261	1.026	-0.5	-116.49	999	Settings of SCR 3 were applied to SCR 20
5	13	20	360	162	41.945	1.043	-0.5	-141.907	9.5	Higher initial WTG terminal voltage

*Settling time of 999 sec indicates inability to recover the POI voltage to the steady state value

5. Summary

Wind farms can be utilized to provide voltage control to the connected network using a supervisory VAR control. This work has presented the development of the VAR control for a large-scale wind farm to control the voltage at the point of interconnection (POI) with the electric grid.

Different types of wind turbine generators (WTGs) have been considered to accommodate present and possible future drivetrain technologies.

- The first type has power electronics interfaces with the electric grid. It includes the doubly fed induction generator (DFIG) machine type (GE 1.5/3.6 MW), which has a partially rated converter. It also includes the synchronous WTG machine (GE 2.5 MW), which is connected to the grid through a full converter. This type of power electronics interface with the grid features fast dynamic response of the WTG voltage.
- The second type is the conventional synchronous machine type, which is directly connected to the grid. It has a longer excitation time constant and therefore, the WTG terminal voltage time response is slower. This type of machine can be implemented with future variable speed drivetrain technologies.

For synchronous machine WTG types, two different excitation systems were investigated. The first one is the static excitation system and the second one is the brushless excitation system, which has a relatively slower time response. Two VAR control strategies were investigated.

- The first strategy had only a WTG voltage control loop. The design does not take into account the machine reactive power capability, which can be exceeded particularly with higher SCR systems. It is worth mentioning that the control parameters should not make the VAR control response faster than that of the WTG excitation system to the extent that can cause voltage collapse with system disturbances, and in these cases the control parameters should be carefully chosen. This is important particularly with the brushless excitation system, which has a slower time response.
- The second VAR control strategy included an additional reactive power control loop, which is vital to respect the machine reactive power capability.

The VAR control design guidelines for each WTG type have been discussed. Test cases have been conducted to show the response of each WTG technology. A criterion for performance evaluation was developed. The main factors affecting the wind farm VAR control were investigated in detail with the following findings:

- The grid short circuit ratio (SCR) level has a major impact on the control design and response.
- Monitoring the number of connected WTGs is important for updating the control parameters. With over 50% of connected WTGs online, the impact is relatively insignificant. However with lower fraction of WTGs online, adapting the control scheme parameters is recommended for more robust control and for achieving roughly the same VAR control time response with different numbers of connected WTGs.
- With well-tuned control parameters, the VAR control performance with the conventional synchronous machines could have similar time responses to that obtained with the DFIG machine type with power electronics grid interface or full power converter interfaces.

6. Acknowledgements

We gratefully acknowledge funding from the European Community with financial participation under the Sixth Framework Programme for the Integrated Wind Turbine Design project (UPWIND), contract number 019945.

7. References

- [1] Upwind Project WP9.4.2 – Electrical Grid, “Design of Large Scale Offshore Wind Farms”, GE-GRC Munich.
- [2] Miller, N.W. Sanchez-Gasca, J.J. Price, W.W. Delmerico, R.W., “Dynamic modelling of GE 1.5 and 3.6 MW wind turbine-generators for stability simulations”, IEEE Power Engineering Society General Meeting, 2003, Vol. 3, pp. 1977- 1983.
- [3] ABB, XLPE Cable Systems, User’s Guide.
- [4] Wind Park Management System (WPMS) Reactive Power Control (WindVAR) Design Guideline, GE Internal Report, September 2004.
- [5] Koessler, R.J., “Techniques for Tuning Excitation System Parameters”, IEEE Trans. Energy Conversion, Vol, 3, No. 4, Dec. 1988, pp. 785-791
- [6] General Electric, Positive Sequence Load Flow (PSLF) Manual.
- [7] IEEE Std. 421.2-1990, “IEEE Guide for Identification, Testing, and Evaluation of the Dynamic Performance of Excitation Control System”.